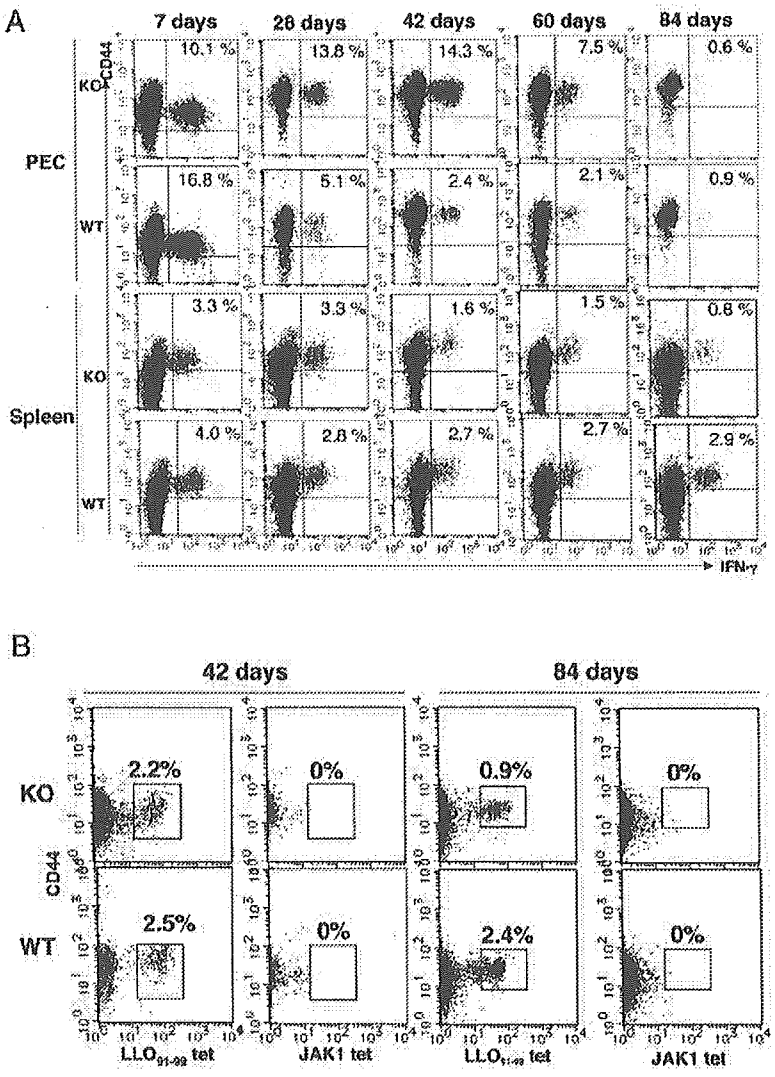

FIGURE 1. CD153 is required for generation of long-lived memory $CD8^+$ T cells. *A*, Kinetics of LLO_{91-99}-specife $CD8^+$ T cells in the peritoneal cavities and spleen of $CD153^{-/-}$ mice and wild-type mice after infection with *L. monocytogenes*. Cells were harvested from $CD153^{-/-}$ mice and wild-type mice infected with 1×10^5 CFU *L. monocytogenes*, washed, and suspended at 10^6 cells/ml in a complete culture medium and were then incubated for 5 h at 37°C in the presence of 10 μg/ml brefeldin A and 5 μg/ml LLO_{91-99} peptide. These cells were harvested, washed, and incubated for 30 min at 4°C with PE-conjugated anti-CD44 mAb, biotin-conjugated CD8 mAb, and then CyChrome-conjugated streptavidin. The cells were stained with FITC-conjugated IFN-γ mAb for 30 min at room temperature, and fluorescence of the cells was analyzed using a flow cytometer. The analysis gate was set on $CD8^+$ T cells. Each number in a quadrant indicates the percentage of each quadrant. Representative results from three separate experiments are shown. *B*, H2-K^d/LLO_{91-99} tetramer-positive $CD8^+$ T cells in the spleens of $CD153^{-/-}$ mice and wild-type mice at 84 days after *L. monocytogenes* infection. For staining of tetrameric H2-K^d-peptide complexes, spleen cells from $CD153^{-/-}$ mice and wild-type mice infected with 1×10^5 *L. monocytogenes* 42 and 84 days previously were incubated at 4°C for 20 min in unconjugated streptavidin (0.5 mg/ml) and Fc block (2.4G2), followed by triple staining with FITC-CD44, CyChrome-CD8α, and PE-conjugated tetrameric H2-K^d/LLO_{91-99} for 30 min at 4°C. The cells were analyzed using a FACSCalibur flow cytometer, and then the analysis gate was set on $CD8^+$ T cells. Each number indicates the percentage of H2-K^d/LLO_{91-99}-positive cells in $CD8^+$ T cells. Representative results from three separate experiments are shown.

after infection at a relatively early stage of memory T cell generation as compared with cells found in wild-type mice, whereas the number of Ag-specific $CD8^+$ T cells in the spleen of $CD153^{-/-}$ mice did not differ from that in wild-type mice on day 28 and had decreased in $CD153^{-/-}$ mice on day 42 after infection (Fig. 1*A*).

Notably, the numbers of LLO_{91-99}-specific $CD8^+$ T cells were significantly decreased in the spleen, LN, and peritoneal cavity of $CD153^{-/-}$ mice on day 84 at a relatively late stage of memory T cell generation compared with those in wild-type mice (Figs. 1 and 2; $p < 0.01$). These results suggest that absence of CD153 in vivo does not affect generation of Ag-specific effector $CD8^+$ T cells but hampers the generation of long-lived memory $CD8^+$ T cells after *L. monocytogenes* infection.

Impaired generation of memory $CD8^+$ T_{CM} cells in $CD153^{-/-}$ mice after Listeria *infection*

The memory T cell compartment can be divided into T_{CM} and T_{EM} cell subsets based on the expression of several cell surface molecules such as LN-homing receptors (3, 4). CD62L expression is useful in distinguishing between these two subsets because T_{CM} cells are mostly $CD62L^{high}$, whereas T_{EM} cells are $CD62L^{low}$ (3, 4). We first examined the expression of CD62L on LLO_{91-99}-specific $CD8^+$ T cells in spleens of wild-type and $CD153^{-/-}$ mice on day 42 after *L. monocytogenes* infection, at which time the number of Ag-specific $CD8^+$ T cells in $CD153^{-/-}$ mice was much more equal to that in wild-type mice. The cells were analyzed by four-color flow cytometory for the simultaneous expression of CD8, CD44, and CD62L on LLO_{91-99}-specific $CD8^+$ T cells. The majority (87%) of LLO_{91-99}-specific $CD8^+$ T cells in $CD153^{-/-}$ mice shown gated in Fig. 3*A* were of the $CD62L^{low}$ phenotype, whereas only 13% were $CD62L^{high}$. In contrast, the memory $CD8^+$ T cells from wild-type mice shown gated in Fig. 4*A* were referred as to $CD62L^{low}$ population (32.2%) and majority $CD62L^{high}$ (67.8%) population. The proportions of $CD62L^{high}$ cells in the LLO_{91-99}-specific $CD8^+$ T cells in the spleen, LNs, and peritoneal cavity of $CD153^{-/-}$ mice were significantly lower than those in wild-type mice on day 42 after infection.

T_{CM} cells exhibit higher proliferative ability than do T_{EM} cells (4). To further confirm impairment of generation of T_{CM} cells in $CD153^{-/-}$ mice following *Listeria* infection, we next analyzed the functional properties of LLO_{91-99}-specific $CD8^+$ T cells from the spleens of wild-type and $CD153^{-/-}$ mice on day 42 after infection in in vitro response to LLO_{91-99} peptide. The ability of $CD8^+$ T cells from $CD153^{-/-}$ mice to produce the IFN-γ was comparable to that of $CD8^+$ T cells from wild-type mice (Fig. 3*B*). However,

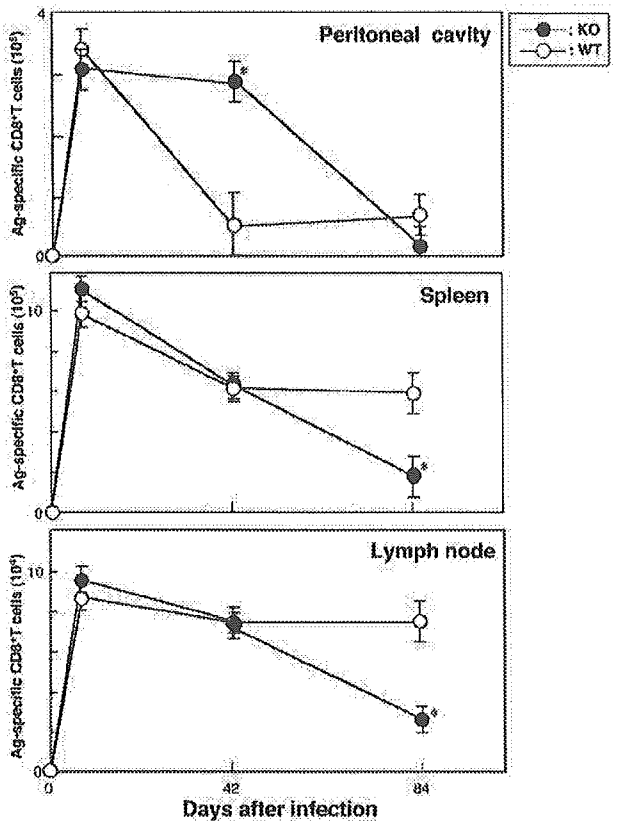

FIGURE 2. Kinetics of absolute numbers of LLO_{91-99}-specific $CD8^+$ T cells in $CD153^{-/-}$ mice and wild-type mice following *L. monocytogenes* infection. The absolute numbers of LLO_{91-99}-specific $CD8^+$ T cells were calculated by multiplying total cells by percentage of LLO_{91-99}-specific $CD8^+$ T cells producing IFN-γ in each organ. Representative results from three separate experiments are shown, and data are expressed as mean ± SD of five mice of each group from the representative experiment. *, $p < 0.05$, significantly different from the value for wild-type mice.

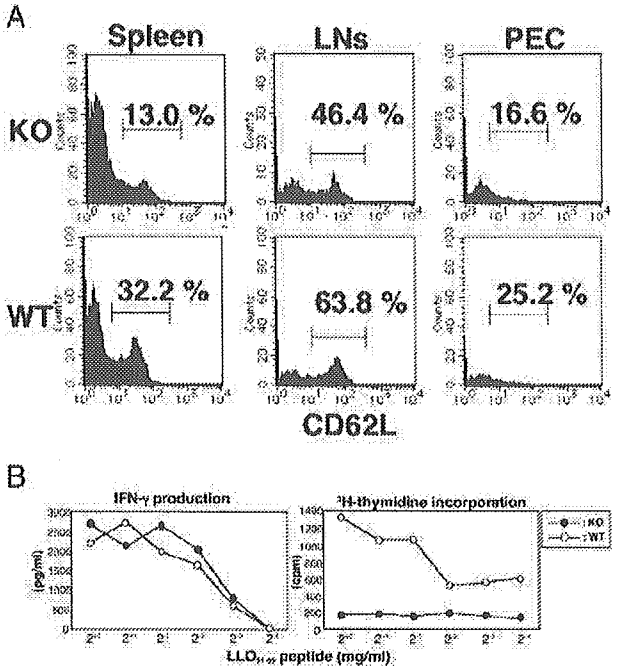

FIGURE 3. Impaired generation of memory $CD8^+$ T_{EM} cells in $CD153^{-/-}$ mice after *Listeria* infection. *A*, CD62L expression on LLO_{91-99}-specific $CD8^+$ T cells in $CD153^{-/-}$ mice and wild-type mice infected with *L. monocytogenes* 42 days previously. LLO_{91-99}-specific $CD8^+$ T cells from $CD153^{-/-}$ mice and wild-type mice at 42 days after infection were costained for CD62L expression. Plots are gated on $CD8^+$ LLO_{91-99} tetramer-positive (tet$^+$) cells. *B*, IFN-γ production and proliferative activity of $CD8^+$ T cells from $CD153^{-/-}$ mice or wild-type mice infected with *L. monocytogenes* 42 days previously. IFN-γ production by $CD8^+$ T cells from $CD153^{-/-}$ mice and wild-type mice at 42 days after infection separated using magnetic beads (95% pure) was assessed by ELISA following LLO_{91-99} peptide stimulation. Proliferative activity of $CD8^+$ T cells from $CD153^{-/-}$ mice and wild-type mice at 42 days after infection was assessed by incorporation of [^{3}H]thymidine. The data are representative of three independent experiments using pooled cells from three $CD153^{-/-}$ or wild-type mice.

only $CD8^+$ T cells from wild-type mice were capable of proliferating in response to LLO_{91-99} peptide (Fig. 3*B*). From these results, it is concluded that $CD8^+$ T_{CM} cells are poorly generated in $CD153^{-/-}$ mice following *L. monocytogenes* infection, although T_{EM} cells accumulated in nonlymphoid tissues at a relatively early stage of memory T cell generation.

Lack of CD153 causes a progressive loss in protective immunity against reinfection with Listeria

As described, the numbers of long-lasting Ag-specific memory $CD8^+$ T cells in both nonlymphoid and lymphoid tissues were greatly decreased on day 84 after *Listeria* infection. We examined the functional relevance of this decrease by analyzing Ag-specific CTL activity in vivo in $CD153^{-/-}$ mice on day 84 after *Listeria* infection. This analysis was done by monitoring the specific eradication of an adoptive transferred target population of LLO_{91-99}-pulsed splenocytes that had been differentially labeled with $CFSE^{high}$ so as to be distinguishable from a cotransferred reference population ($CFSE^{low}$). Fig. 4*A* shows that strong and specific cytotoxic effectors were detectable in the spleens of infected wild-type mice. In contrast, the numbers of CTLs in $CD153^{-/-}$ mice were greatly decreased on day 84 after infection with *L. monocytogenes* (Fig. 4*A*). The loss of functional CTL activity in $CD153^{-/-}$ mice might be results of quantitative, but not qualitative, decrease by the Ag-specific $CD8^+$ T cells because the number of tetrameric H2-K^d/LLO_{91-99}-positive cells was significantly decreased in the $CD153^{-/-}$ mice on day 84 after infection compared with the number of cells in wild-type mice (Fig. 2).

To evaluate protective immunity against *L. monocytogenes* in wild-type and $CD153^{-/-}$ mice inoculated with *Listeria* 84 days previously, we tested the ability to control a lethal challenge of *L. monocytogenes* (1×10^6 CFU). As expected, LLO_{91-99}-specific $CD8^+$ T cells poorly expanded in $CD153^{-/-}$ mice compared with those in wild-type mice on day 5 after a secondary challenge (Fig. 4*B*). There was no difference in the number of bacteria in the spleen and liver of between unimmunized $CD153^{-/-}$ and wild-type mice (Fig. 4*C*). However, consistent with the results of levels of memory CD8 T cells, there was a marked deficiency in the protection of $CD153^{-/-}$ mice against lethal challenge with *L. monocytogenes* (Fig. 4*C*). Collectively, $CD153^{-/-}$ mice poorly generated long-lived memory $CD8^+$ T cells, which were not able to lyse peptide-coated target cells and were not able to confer protective immunity against reinfection. Although T_{EM} cells had accumulated in the $CD153^{-/-}$ mice on day 42 after infection, the mice poorly generated long-lived memory $CD8^+$ T cells at a later stage of infection. This result suggests that T_{CM} cells may be important for generation of long-lived memory $CD8^+$ T cells following Ag exposure.

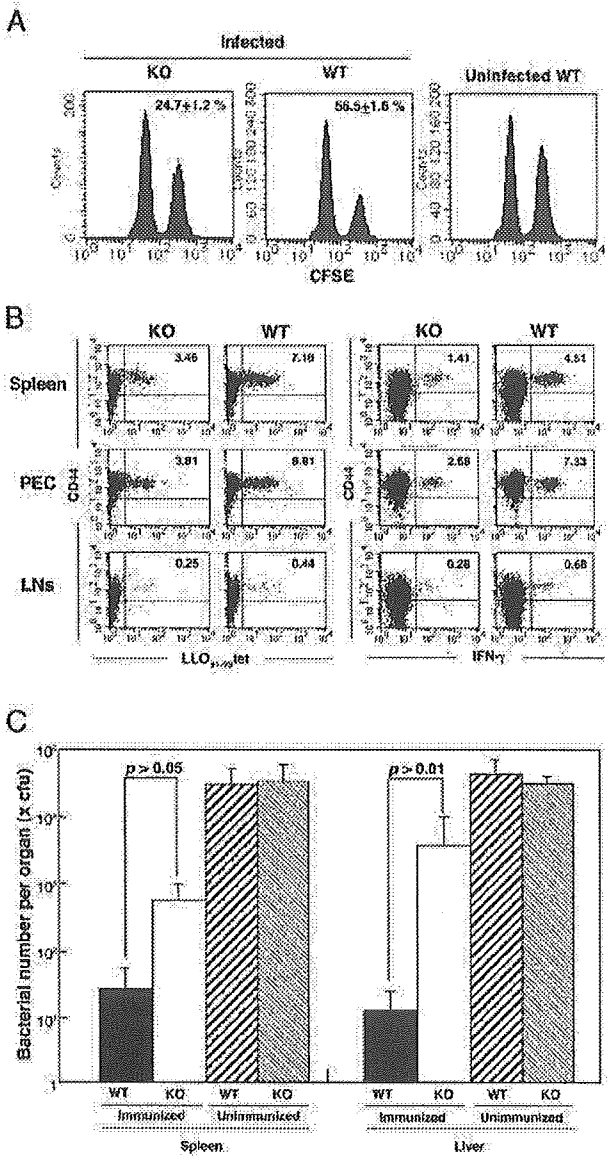

FIGURE 4. Lack of CD153 causes a progressive loss in protective immunity against reinfection with *Listeria*. *A*, Cytotoxic responses of $CD8^+$ T cells in $CD153^{-/-}$ mice and wild-type mice at 84 days after *L. monocytogenes* infection. In vivo killing of LLO_{91-99} peptide-pulsed target cells labeled with $CFSE^{high}$ in uninfected mice, wild-type mice and $CD153^{-/-}$ mice at 84 days after infection was determined by monitoring the specific eradication of an adoptive transferred target population of LLO_{91-99}-pulsed splenocytes that had been differentially labeled with $CFSE^{high}$ so as to be distinguishable from a cotransferred reference population ($CFSE^{low}$). The number shown represents the percentage of specific killing to that of control $CFSE^{low}$-labeled cells (mean ± SD; $n = 5$). *B*, Expansion of LLO_{91-99}-specific $CD8^+$ T cells in $CD153^{-/-}$ mice and wild-type mice on day 5 after secondary challenge. Tetrameric H2-K^d-peptide complexes or intracellular cytokine staining of LLO_{91-99}-specific $CD8^+$ T cells in $CD153^{-/-}$ mice and wild-type mice were examined by flow cytometry and analyzed by gating on $CD8^+$ T cells. *C*, Protection against lethal challenges with *L. monocytogenes* in $CD153^{-/-}$ mice and wild-type mice infected with *L. monocytogenes* 84 days previously. $CD153^{-/-}$ mice and wild-type mice that had each been infected with 1×10^5 CFU *L. monocytogenes* 84 days previously were each challenged with a lethal dose of *L. monocytogenes* (1×10^6 CFU), the numbers of bacteria in spleens and livers were counted 2 days later. Each column and vertical bar represent mean ± SD of five mice in each group. *, $p < 0.05$, significant difference between the values for wild-type CD8 to BALB/c and the values for immune $CD153^{-/-}$ CD8 T cells to BALB/c.

CD30L signaling induces CCR7 expression in T_{EM}

We found that long-lasting $CD8^+$ T_{CM} cells are poorly generated in $CD153^{-/-}$ mice, whereas $CD8^+$ T_{EM} cells accumulate in nonlymphoid tissues at a relatively early stage of memory T cell generation after *L. monocytogenes* infection. Furthermore, we previously found by DNA chip analysis that CD30 signaling up-regulates CCR7 mRNA (23, 24). These findings give rise to the possibility that CD30 signaling makes T_{CM} cells by inducing expression of LN-homing receptors, including CCR7. To address this issue, we first examined changes in expression of LN-homing receptors of purified $CD62L^+CD44^+CD8^+$ T_{EM} after CD30 stimulation. The purified $CD62L^+CD44^+CD8^+$ T_{EM} cells were stimulated with plate-bound CD30 mAb for 24 h. We first examined the expression of CD62L on the surfaces of T_{EM} cells after anti-CD30 mAb cross-linking, but T_{EM} cells did not express CD62L molecules after stimulation. We next examined gene expression of chemokine receptors, including CCR5, CCR6, and CCR7, in the T_{EM} cells stimulated with anti-CD30 mAb. As shown in Fig. 5 after anti-CD30 mAb cross-linking, the gene expression of CCR7 was greatly up-regulated and the gene expression of CCR5 was down-regulated in T_{EM} cells. These results suggest that CD30/CD30L signaling may play an important role in the generation of long-lived memory $CD8^+$ T cells after Ag exposure by triggering the expression of CCR7 in T_{EM} cells to make them migrate and differentiate into T_{CM} cells in nonlymphoid organs.

These results suggest that CD30/CD30L signaling plays an important role in the differentiation of T_{CM} cells through induction of CCR7 mRNA expression.

Discussion

In the present study, we found that CD30/CD30L signaling is involved in differentiation of long-lived $CD8^+$ T_{CM} cells following exposure to a microbe. Although $CD8^+$ T_{EM} cells transiently accumulated in the nonlymphoid tissues of $CD153^{-/-}$ mice after *Listeria* infection, long-lived $CD8^+$ T_{CM} cells, which exhibit strong proliferative ability and play a role in protective immunity, were generated in only small numbers in these mice following *Listeria* infection. These results suggest that CD30/CD30L signaling may play an important role in the generation of long-lived $CD8^+$ T_{CM} cells after exposure to a microbe.

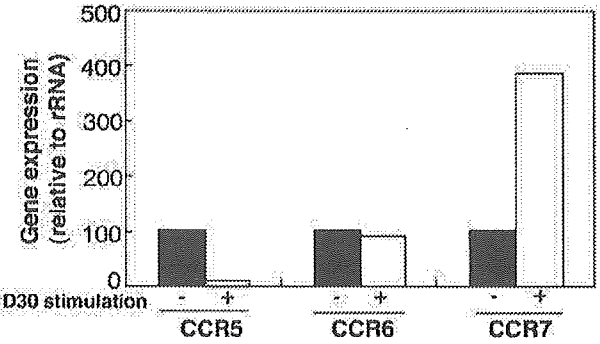

FIGURE 5. CD30L signaling induces CCR7 expression in T_{EM} cells. Up-regulation of CCR7 expression in T_{EM} cells in response to CD30 cross-linking. Purified $CD62L^+CD44^+CD8^+$ T_{EM} cells were stimulated with plate-bound anti-CD30 mAb (clone CD30.1) for 24 h. Gene expressions of the chemokine receptors CCR5, CCR6, and CCR7 in T_{EM} cells stimulated with anti-CD30 mAb were examined by quantitative RT-PCR. First-strand cDNA was synthesized with random primers. cDNA encoding chemokine receptors were analyzed by real-time PCR using a TaqMan PCR kit and an ABI PRISM 7000 sequence detector thermal cycler according to the recommended protocol of the manufacturer (Applied Biosystems). Data of gene expression were normalized on the basis of rRNA mRNA levels. Representative results from three separate experiments are shown.

Upon encounter with a pathogenic microbe, Ag-specific T cells proliferate and differentiate into activated effector T cells. Most of the activated T cells die by apoptosis (31), but the few that survive become memory cells and persist for a long period of time, sometimes throughout the life of an animal (32–34). Memory is dependent on the amount of surviving T cells after primary TCR-mediated activation and presumably on escape from activation-induced cell death or starvation cell death by apoptosis (35). It has been recently reported that naive CD8$^+$ T cells receiving prolonged or strong stimulation of T cell receptors can differentiate into effector cells and survive as memory T cells by enhancing IL-15/IL-7 responsiveness (36). TNF/TNFR superfamily is known to play important roles in generation of effector T cells as accessory molecules during an immune response (6). CD153 has been detected on activated mouse DCs (16). Therefore, the CD153-CD30 pair may contribute to T cell priming at dendritic cell-T cell interaction like 4-1BB and OX40 (37–39). In addition, CD153 is expressed on activated T cells and can support T cell expansion during T-T cell interaction (37). There are several lines of evidence that CD4 help is important for generation of memory CD8 T cells following microbial infection (40). Therefore, it is possible that defective dendritic cell and T cell help may account for the altered CD8 T cell responses in CD153$^{-/-}$ mice. However, the results of the present study indicate that the generation of effector CD8$^+$ T cells seems to occur normally in CD153$^{-/-}$ mice at induction phase of effector T cells after *Listeria* infection. Furthermore, the number of T_{EM} cells increased, albeit transiently, after *Listeria* infection in CD30/CD30L$^{-/-}$ mice. CD30/CD30L signaling might not be essential at least for the generation of effector CD8$^+$ T cells and CD8 T_{EM} cells after exposure to a microbe.

Because both T_{CM} and T_{EM} cells can be generated during the same immune response to *L. monocytogenes*, a key question is how these subpopulations are related to each other. Recent studies have provided new insights into the lineage relationship between T_{CM} and T_{EM} cells (1–3). There is evidence suggesting that T_{EM} cells can convert into T_{CM} cells under appropriate in vivo conditions (4). The numbers of T_{EM} and T_{CM} cells changed substantially over time and did so in a reciprocal manner, with the number of T_{CM} cells increasing and the number of T_{EM} cells decreasing. Wherry et al. (4) investigated this possibility directly by transferring purified populations of T_{EM} cells or T_{CM} cells into secondary recipients and examining the fate of the transferred cells. These researchers found that T_{CM} cells retained their phenotype for at least 30 days after transfer, whereas half of the T_{EM} cells acquired the phenotype of T_{CM} cells during this period. They therefore proposed a linear differentiation model of a memory CD8$^+$ T cell subset. In the present study, the generation of T_{CM} cells was impaired in the absence of CD30L/CD30 signaling following *Listeria* infection in vivo, and an LN-homing receptor, CCR7, was strongly up-regulated in T_{EM} cells after anti-CD30 mAb cross-linking in vitro. On the basis of the linear differentiation theory, our results suggest that CD30/CD30L signaling plays an important role in the generation of long-lived memory CD8$^+$ T cells after exposure to an Ag by triggering differentiation into T_{CM} cells via induction of the expression of CCR7 on T_{EM} cells in nonlymphoid organs. In contrast, in the case of CD8$^+$ T cells, there is some evidence that T_{CM} and T_{EM} cells might be generated differentially during an immune response depending on the conditions of activation (5, 41). On the basis of the different lineage theory that CD8$^+$ T_{CM} and T_{EM} cells are largely independent subpopulations, the possibility that fewer CD8$^+$ T_{CM} cells are generated in the absence of CD30L/CD30 signaling at the time of immune response after primary infection with *L. monocytogenes* cannot be excluded.

It is notable that CD8$^+$ T_{EM} cells transiently accumulated in nonlymphoid tissues in CD153$^{-/-}$ mice at a relatively early stage of the memory phase. *L. monocytogenes* was eliminated both in CD153$^{-/-}$ mice and wild-type mice in $\leq$10 days after infection, but preferential accumulation of T_{EM} cells in CD153$^{-/-}$ mice was still observed on day 42 after infection with *L. monocytogenes*. It is possible that T_{EM} cells can survive in nonlymphoid tissues for several weeks in the absence of a relevant Ag or CD30L. According to the linear differentiation theory, CD30/CD30L signaling is essential for conversion of T_{EM} cells into T_{CM} cells at least partly via induction of CCR7 expression. Memory T cells in nonlymphoid tissues may express CCR7 by CD30L/CD30 signaling and then migrate to lymphoid tissues with abundant expression of ligands for CCR7 such as secondary lymphoid-tissue chemokine. Because of the lack of CCR7 expression by CD30/CD30L signaling, T_{EM} cells may remain in nonlymphoid tissues of CD153$^{-/-}$ mice, resulting in preferential accumulation of T_{EM} cells in the nonlymphoid tissues. Alternatively, according to a different lineage theory, T_{EM} cells may be preferentially generated in lymphoid tissues in the absence of CD30L and migrate to nonlymphoid tissues due to the lack of CCR7 expression, resulting in accumulation of T_{EM} cells in nonlymphoid tissues of CD153$^{-/-}$ mice after infection.

CD30 has been reported to be preferentially expressed by Th2 and T cytotoxic type-2 (Tc2) cells (5, 14, 42–44), and blocking of CD30L/CD30 signaling has been reported to suppress the development of Th2 cells and to enhance the development of Th1 cells in vitro (45). These results suggest that CD30L/CD30 signaling plays a role in the proliferation, cytokine secretion, and survival of Th2 cells, although controversy results have been reported (46). Tc1 and Tc2 cells are known to mutually regulate in their differentiation, and Th1 cells have been reported to be subjected to apoptosis weaker than Tc2 cells (7, 31) Therefore, it is alternatively possible that Tc2 cells producing IL-4 are selectively suppressed after infection in CD153$^{-/-}$ mice, resulting in preferential accumulation of memory Tc1 cells in nonlymphoid tissues at a relatively early stage of the memory phase. However, our results of intracellular IFN-γ FACS staining and tetramer staining revealed that the number of Ag-specific CD8$^+$ Tc1 cells in CD153$^{-/-}$ mice did not increase at the peak of a primary response in CD153$^{-/-}$ mice. Furthermore, memory Tc2 cells were never detected in wild-type mice following *Listeria* infection (data not shown). Deviation from Tc2 cells to Tc1 cells in CD30L-deficient mice may not be due to an increase in the number of memory CD8$^+$ T_{EM} cells.

The principal attribution of memory T cells is their ability to undergo cell division called "homeostatic proliferation" to maintain their number (1, 47). Homeostatic proliferation is thought to be required for the long-term maintenance of Ag-driven memory CD8$^+$ T cells in vivo. A T_{EM} cell population that is CCR7$^-$CD62L^{low} has little homeostatic proliferative potential, and this subset therefore does not seem to be a permanent memory population (4). In contrast, a T_{CM} cell subset that is CCR7$^+$CD62L^{high} is capable of efficient homeostatic proliferation and may survive for a long time in lymphoid tissues (4). In the present study, memory CD8$^+$ T cells in both lymphoid and nonlymphoid tissues of CD153$^{-/-}$ mice decreased dramatically at the late stage of infection. Most of the memory T_{EM} cells in nonlymphoid tissues of CD153$^{-/-}$ mice might die by apoptosis due to the lack of their responsiveness to survival signals or survival signals themselves. Recent studies have suggested that cytokines such as IL-15/IL-7 are involved in the proliferation and survival of Ag-driven memory CD8$^+$ T cells in the absence of Ag (48–53).

The TNFR-associated factor (TRAF)-linked TNFR family members CD40, OX40, 4-1BB, and CD27 by virtue of their anti-apoptotic effects, would be prime candidates to shape T cell memory (6). These molecules might be responsible for maintenance of T_{CM} cells in the lymphoid tissues. It has recently been reported that $CD4^+CD3^-$ accessory cells have low levels of CD80 or CD86 expression but express high levels of the two TNF ligands OX40 ligand and CD153 in the B cell area of lymphoid tissues (16). OX40 has been found to up-regulate expression of the CXC chemokine receptor (CXCR) 5 and allows T cell migration into B cell areas of peripheral lymphoid organs (54). We found that CD30 stimulation also induced CXCR5 expression on T_{EM} cells (our unpublished observation). Therefore, it is possible that CD30 signaling up-regulates the expression of CCR7 and CXCR5 on memory T cells, enabling these T cells to migrate to B cells areas of lymphoid tissues. Survival signaling from $CD4^+CD3^-$ accessory cells in lymphoid tissues may play an important role in the maintenance of T_{CM} cells for a long period. It is also possible that CD30 signaling provides direct survival signal or the responsiveness to memory $CD8^+$ T cells in addition to up-regulation of the expression of homing receptors. CD30 uses TRAF molecules, particularly TRAF2 and TRAF5, to induce downstream signals (55–57). TRAF2 is thought to be responsible for NF-κB activation and for the antiapoptotic effect mediated by CD30 (55–57). Although lymphocyte homeostasis does not seem to be affected in $TRAF5^{-/-}$ mice, $TRAF2^{-/-}$ mice are severely lymphopenic, suggesting that this molecule plays a role in T and B cell survival (58, 59). Analysis of the virus-specific response of $CD4^+$ T cells isolated from the spleen of immunized mice confirmed that CD30 is essential for adequate expansion of Ag-activated T cells. It is still unclear whether CD153 expression is required for maintenance or emergence of $CD62L^{high}$ cells at the late stage after *Listeria* infection.

We showed that CCR7 expression was up-regulated by CD30 stimulation in $CD62L^-CD44^+CD8^+$ T_{EM} cells. In this respect, it should be noted that triggering through the TCR has been shown to result in both down-regulation of CCR7 expression on CD8 T_{CM} cells and up-regulation of CCR7 expression in CD8 T_{EM} cells (36). We previously showed by gene microarray analysis strong up-regulation of CCR7 in large granular lymphocyte lymphoma by CD30 (23, 24). We found that CD30, but not other TRAF2 involving molecules containing CD40 and IL-15Rα induced CCR7 expression in the $CD62L^-$ $CD44^+CD8^+$ T_{EM} cells (our unpublished observations) (Fig. 5*A*). These results suggest that other signaling such as by the MAPK pathway may be involved in the up-regulation of CCR7 on memory $CD8^+$ T cells. Further analysis is needed to elucidate the effects of CD30 signaling on memory $CD8^+$ T cells. It is also interesting whether CCR7 expression level in naive $CD8^+$T cells is altered in $CD153^{-/-}$ mice. However, homing of naive $CD8^+$ T cells in CD153-deficient mice was not affected. CD153 is expressed by activated dendritic cells, and CD30 is expressed by activated and memory $CD8^+$ T cells but not by naive $CD8^+$ T cells (6, 14–16). Therefore, CD30L/CD30 signaling for up-regulation of CCR7 may only serve to function on activated/memory $CD8^+$ T cells.

In conclusion, we have shown that CD30/CD30L signaling is involved in the expression of CCR7 in T_{EM} cells following *Listeria* infection. Ag-specific T_{EM} cells accumulated preferentially in $CD153^{-/-}$ mice at the early stage of *L. monocytogenes* infection. In contrast, long-lived memory $CD8^+$ T cells, which function in protective immunity, were not generated in large numbers in $CD153^{-/-}$ mice at the later stage of infection. These results suggest that CD30/CD30L signaling plays an important role in the generation of long-lived memory $CD8^+$ T cells after exposure to an Ag by triggering differentiation into T_{CM} cells via induction of expression of CCR7 on T_{EM} cells in nonlymphoid organs.

Acknowledgments

We thank K. Kaneda, Y. Kobayashi, and S. Takashima for technical assistance.

Disclosures

The authors have no financial conflict of interest.

References

1. Kaech, S. M., E. J. Wherry, and R. Ahmed. 2002. Effector and memory T-cell differentiation: implications for vaccine development. *Nat. Rev. Immunol.* 2: 251–262.
2. Lanzavecchia, A., and F. Sallusto. 2000. Dynamics of T lymphocyte responses: intermediates, effectors, and memory cells. *Science* 290: 92–97.
3. Sallusto, F., D. Lenig, R. Forster, M. Lipp, and A. Lanzavecchia. 1999. Two subsets of memory T lymphocytes with distinct homing potentials and effector functions. *Nature* 401: 708–712.
4. Wherry, E. J., V. Teichgraber, T. C. Becker, D. Masopust, S. M. Kaech, R. Antia, U. H. von Andrian, and R. Ahmed. 2003. Lineage relationship and protective immunity of memory CD8 T cell subsets. *Nat. Immunol.* 4: 225–234.
5. Weninger, W., M. A. Crowley, N. Manjunath, and U. H. von Andrian. 2001. Migratory properties of naive, effector, and memory $CD8^+$ T cells. *J. Exp. Med.* 194: 953–966.
6. Croft, M. 2003. Co-stimulatory members of the TNFR family: keys to effective T-cell immunity? *Nat. Rev. Immunol.* 3: 609–620.
7. Hildeman, D. A., Y. Zhu, T. C. Mitchell, J. Kappler, and P. Marrack. 2002. Molecular mechanisms of activated T cell death in vivo. *Curr. Opin. Immunol.* 14: 354–359.
8. Bourgeois, C., B. Rocha, and C. Tanchot. 2002. A role for CD40 expression on $CD8^+$ T cells in the generation of $CD8^+$ T cell memory. *Science* 297: 2060–2063.
9. Janssen, E. M., E. E. Lemmes, T. Wolfe, U. Christen, M. G. von Herrath, and S. P. Schoenberger. 2003. $CD4^+$ T cells are required for secondary expansion and memory in $CD8^+$ T lymphocytes. *Nature* 421: 852–856.
10. Shedlock, D. J., and H. Shen. 2003. Requirement for CD4 T cell help in generating functional CD8 T cell memory. *Science* 300: 337–339.
11. Sun, J. C., and M. J. Bevan. 2003. Defective CD8 T cell memory following acute infection without CD4 T cell help. *Science* 300: 339–342.
12. Dürkop, H., U. Latza, M. Hummel, F. Eitelbach, B. Seed, and B. Stein. 1993. Molecular cloning and expression of a new member of the nerve growth factor receptor family that is characteristic for Hodgkin's disease. *Cell* 68: 421–427.
13. Ellis, T. M., P. E. Simms, D. J. Slivnick, H.-M. Jack, and R. J. Fisher. 1993. CD30 is a signal-transducing molecule that defines a subset of human activated $CD45RO^+$ T cells. *J. Immunol.* 151: 2380–2389.
14. Bowen, M. A., R. K. Lee, G. Miragliotta, S. Y. Nam, and E. R. Podack. 1996. Structure and expression of murine CD30 and its role in cytokine production. *J. Immunol.* 156: 442–449.
15. Smith, C. A., H. J. Gruss, T. Davis, D. Anderson, T. Farrah, E. Baker, G. R. Sutherland, C. I. Brannan, N. G. Copeland, N. A. Jenkins, et al. 1993. CD30 antigen, a marker for Hodgkin's lymphoma, is a receptor whose ligand defines an emerging family of cytokine with homology to TNF. *Cell* 73: 1349–1360.
16. Kim, M.-Y., F. M. C. Gaspal, H. E. Wiggett, F. M. McConnell, A. Gulbranson-Judge, C. Raykundalia, L. S. K. Walker, M. D. Goodall, and P. J. L. Lane. 2003. $CD4^+CD3^-$ accessory cells costimulate primed CD4 T cells through OX40 and CD30 at sites where T cells collaborate with B cells. *Immunity* 18: 643–654.
17. Kurts, C., F. R. Carbone, M. F. Krummel, K. M. Koch, J. F. A. P. Miller, and W. R. Heath. 1999. Signalling through CD30 protects against autoimmune diabetes mediated by CD8 T cells. *Nature* 398: 341–344.
18. Amakawa, R., A. Hakem, T. M. Kundig, T. Matsuyama, J. J. Simard, E. Timms, A. Wakeham, H. W. Mittruecker, H. Griesser, H. Takimoto, et al. 1996. Impaired negative selection of T cells in Hodgkin's disease antigen CD30-deficient mice. *Cell* 84: 551–562.
19. Telford, W. G., S. Y. Nam, E. R. Podack, and R. A. Miller. 1997. CD30-regulated apoptosis in murine CD8 T cells after cessation of TCR signaling. *Cell. Immunol.* 182: 125–136.
20. Bowen, M. A., K. J. Olsen, L. Cheng, D. Avila, and E. R. Podack. 1993. Functional effects of CD30 on a large granular lymphoma cell line, YT: inhibition of cytotoxicity, regulation of CD28 and IL-2R, and induction of homotypic aggregation. *J. Immunol.* 151: 5896–5906.
21. Lee, S. Y., S. Y. Lee, G. Kandala, M. L. Liou, H. C. Liou, and Y. Choi. 1996. CD30/TNF receptor-associated factor interaction: NF-κB activation and binding specificity. *Proc. Natl. Acad. Sci. USA* 93: 9699–9703.
22. Lee, S. Y., S. Y. Lee, and Y. Choi. 1997. TRAF-interacting protein (TRIP): a novel component of the tumor necrosis factor receptor (TNFR)- and CD30-TRAF signaling complexes that inhibits TRAF2-mediated NF-κB activation. *J. Exp. Med.* 185: 1275–1285.
23. Muta, H., L. H. Boise, L. Fang, and E. R. Podack. 2000. CD30 signals integrate expression of cytotoxic effector molecules, lymphocyte trafficking signals, and signals for proliferation and apoptosis. *J. Immunol.* 165: 5105–5111.
24. Podack, E. R., N. Strbo, V. Sotosec, and H. Muta. 2002. CD30: governor of memory T cells? *Ann. NY Acad. Sci.* 975: 101–113.

25. Altman, J. D., P. A. Moss, P. J. Goulder, D. H. Barouch, M. G. McHeyzer-Williams, J. I. Bell, A. J. McMichael, and M. M. Davis. 1996. Phenotypic analysis of antigen-specific T lymphocytes. *Science* 274: 94–96.
26. Busch, D. H., I. M. Pilip, S. Vijh, and E. G. Pamer. 1998. Coordinate regulation of complex T cell populations responding to bacterial infection. *Immunity* 8: 353–362.
27. Vijh, S., and E. G. Pamer. 1997. Immunodominant and subdominant CTL responses to *Listeria monocytogenes* infection. *J. Immunol.* 158: 3366–3371.
28. Falk, K., O. Rötzschke, S. Stevanović, G. Jung, and H.-G. Rammensee. 1991. Allele-specific motifs revealed by sequencing of self-peptides eluted from MHC molecules. *Nature* 351: 290–296.
29. Coles, R. M., S. N. Mueller, W. R. Heath, F. R. Carbone, and A. G. Brooks. 2002. Progression of armed CTL from draining lymph node to spleen shortly after localized infection with herpes simplex virus 1. *J. Immunol.* 168: 834–838.
30. Mueller, S. N., C. M. Jones, C. M. Smith, W. R. Heath, and F. R. Carbone. 2002. Rapid cytotoxic T lymphocyte activation occurs in the draining lymph nodes after cutaneous herpes simplex virus infection as a result of early antigen presentation and not the presence of virus. *J. Exp. Med.* 195: 651–656.
31. Lenardo, M., K. M. Chan, F. Hornung, H. McFarland, R. Siegel, J. Wang, and L. Zheng. 1999. Mature T lymphocyte apoptosis: immune regulation in a dynamic and unpredictable antigenic environment. *Annu. Rev. Immunol.* 17: 221–253.
32. Murali-Krishna, K., J. D. Altman, M. Suresh, D. J. D. Sourdive, A. J. Zajac, J. D. Miller, J. Slansky, and R. Ahmed. 1998. Counting antigen-specific CD8 T cells: a reevaluation of bystander activation during viral infection. *Immunity* 8: 177–187.
33. Opferman, J. T., B. T. Ober, and P. G. Ashton-Rickardt. 1999. Linear differentiation of cytotoxic effectors into memory T lymphocytes. *Science* 283: 1745–1748.
34. Jacob, J., and D. Baltimore. 1999. Modelling T-cell memory by genetic marking of memory T cells in vivo. *Nature* 399: 593–597.
35. Badovinac, V. P., B. B. Porter, and J. T. Harty. 2002. Programmed contraction of CD8$^+$ T cells after infection. *Nat. Immunol.* 3: 619–626.
36. Gett, A. V., F. Sallusto, A. Lanzavecchia, and J. Geginat. 2003. T cell fitness determined by signal strength. *Nat. Immunol.* 4: 355–360.
37. Shimozato, O., K. Takeda, H. Yagita, and K. Okumura. 1999. Expression of CD30 ligand (CD153) on murine activated T cells. *Biochem. Biophys. Res. Commun.* 256: 519–526.
38. Vinay, D. S., and B. S. Kwon. 1998. Role of 4-1BB in immune responses. *Semin. Immunol.* 10: 481–489.
39. Weinberg, A. D., A. T. Vella, and M. Croft. 1998. OX-40: life beyond the effector T cell stage. *Semin. Immunol.* 10: 471–480.
40. Rocha, B., and C. Tanchot. 2004. Towards a cellular definition of CD8$^+$ T-cell memory: the role of CD4$^+$ T-cell help in CD8$^+$ T-cell responses. *Curr. Opin. Immunol.* 16: 259–263.
41. Manjunath, N., P. Shankar, J. Wan, W. Weninger, M. A. Crowley, K. Hieshima, T. A. Springer, X. Fan, H. Shen, J. Lieberman, and U. H. von Andrian. 2001. Effector differentiation is not prerequisite for generation of memory cytotoxic T lymphocytes. *J. Clin. Invest.* 108: 871–878.
42. Del Prete, G., M. De Carli, F. Almerigogna, C. K. Daniel, M. M. D'Elios, G. Zancuoghi, F. Vinante, G. Pizzolo, and S. Romagnani. 1995. Preferential expression of CD30 by human CD4$^+$ T cells producing Th2-type cytokines. *FASEB J.* 9: 81–86.
43. Horie, R., and T. Watanabe. 1998. CD30: expression and function in health and disease. *Semin. Immunol.* 10: 457–470.
44. Gerli, R., C. Lunardi, F. Vinante, O. Bistoni, G. Pizzolo, and C. Pitzalis. 2001. Role of CD30$^+$ T cells in rheumatoid arthritis: a counter-regulatory paradigm for Th1-driven diseases. *Trends Immunol.* 22: 72–77.
45. Nakamura, T., R. K. Lee, S. Y. Nam, P. Al-Ramadi, P. A. Koni, K. Bottomly, E. R. Podack, and R. A. Flavell. 1997. Reciprocal regulation of CD30 expression on CD4$^+$T cells by IL-4 and IFN-γ. *J. Immunol.* 158: 2090–2098.
46. Hamann, D., C. M. Hilkens, J. L. Grogan, S. M. Lens, M. L. Kapsenberg, M. Yazdanbakhsh, and R. A. van Lier. 1996. CD30 expression does not discriminate between human Th1- and Th2-type T cells. *J. Immunol.* 156: 1387–1391.
47. Grossman, Z., B. Min, M. Meier-Schellersheim, and W. E. Paul. 2004. Concomitant regulation of T-cell activation and homeostasis. *Nat. Rev. Immunol.* 4: 387–395.
48. Nishimura, H., T. Yajima, Y. Naiki, H. Tsunobuchi, M. Umemura, K. Itano, T. Matsuguchi, M. Suzuki, P. S. Ohashi, and Y. Yoshikai. 2000. Differential roles of interleukin 15 mRNA isoforms generated by alternative splicing in immune responses in vivo. *J. Exp. Med.* 191: 157–170.
49. Yajima, T., H. Nishimura, R. Ishimitsu, T. Watase, D. H. Busch, E. G. Pamer, H. Kuwano, and Y. Yoshikai. 2002. Overexpression of IL-15 in vivo increases antigen-driven memory CD8$^+$ T cells following a microbe exposure. *J. Immunol.* 168: 1198–1203.
50. Tan, J. T., B. Ernst, W. C. Kieper, E. LeRoy, J. Sprent, and C. D. Surh. 2002. Interleukin (IL)-15 and IL-7 jointly regulate homeostatic proliferation of memory phenotype CD8$^+$ cells but are not required for memory phenotype CD4$^+$ cells. *J. Exp. Med.* 195: 1523–1532.
51. Kieper, W. C., J. T. Tan, B. Bondi-Boyd, L. Gapin, J. Sprent, R. Ceredig, and C. D. Surh. 2002. Overexpression of interleukin (IL)-7 leads to IL-15-independent generation of memory phenotype CD8$^+$ T cells. *J. Exp. Med.* 195: 1533–1539.
52. Becker, T. C., E. J. Wherry, D. Boone, K. Murali-Krishna, R. Antia, A. Ma, and R. Ahmed. 2002. Interleukin 15 is required for proliferative renewal of virus-specific memory CD8 T cells. *J. Exp. Med.* 195: 1541–1548.
53. Judge, A. D., X. Zhang, H. Fujii, C. D. Surh, and J. Sprent. 2002. Interleukin 15 controls both proliferation and survival of a subset of memory-phenotype CD8$^+$ T cells. *J. Exp. Med.* 196: 935–946.
54. Obermeier, F., H. Schwarz, N. Dunger, U. G. Strauch, N. Grunwald, J. Schölmerich, and W. Falk. 2003. OX40/OX40L interaction induces the expression of CXCR5 and contributes to chronic colitis induced by dextran sulfate sodium in mice. *Eur. J. Immunol.* 33: 3265–3274.
55. McDonald, P. P., M. A. Cassatella, A. Bald, E. Maggi, S. Romagnani, H. J. Gruss, and G. Pizzolo. 1995. CD30 ligation induces nuclear factor-κB activation in human T cell lines. *Eur. J. Immunol.* 25: 2870–2876.
56. Ansieau, S., I. Scheffrahn, G. Mosialos, H. Brand, J. Duyster, K. Kaye, J. Harada, B. Dougall, G. Hubinger, E. Kieff, et al. 1996. Tumor necrosis factor receptor-associated factor (TRAF)-1, TRAF-2, and TRAF-3 interact in vivo with the CD30 cytoplasmic domain; TRAF-2 mediates CD30-induced nuclear factor κB activation. *Proc. Natl. Acad. Sci. USA* 93: 14053–14058.
57. Aizawa, S., H. Nakano, T. Ishida, R. Horie, M. Nagai, K. Ito, H. Yagita, K. Okumura, J. Inoue, and T. Watanabe. 1997. Tumor necrosis factor receptor-associated factor (TRAF) 5 and TRAF2 are involved in CD30-mediated NFκB activation. *J. Biol. Chem.* 272: 2042–2045.
58. Yeh, W. C., A. Shahinian, D. Speiser, J. Kraunus, F. Billia, A. Wakeham, J. L. de la Pompa, D. Ferrick, B. Hum, N. Iscove, et al. 1997. Early lethality, functional NF-κB activation, and increased sensitivity to TNF-induced cell death in TRAF2-deficient mice. *Immunity* 7: 715–725.
59. Nakano, H., S. Sakon, H. Koseki, T. Takemori, K. Tada, M. Matsumoto, E. Munechika, T. Sakai, T. Shirasawa, H. Akiba, et al. 1999. Targeted disruption of Traf5 gene causes defects in CD40- and CD27-mediated lymphocyte activation. *Proc. Natl. Acad. Sci. USA* 96: 9803–9808.

Tozuka, Y. et al. : Neuron, 47 : 803-815, 2005

学習することが神経細胞を増やすコツ？

戸塚祐介，久恒辰博

脳を鍛え，知的能力をアップさせ，もっと幸せな人生を送りたいと誰しも思う．経験的に，学べば学ぶほど，頭の働きがよくなることが知られているが，その中身についてはほとんどわかっていなかった．今回，学習することで，海馬においてある種の神経細胞（新生ニューロン）の数が増加していることがわかってきた．脳の中で海馬は，記憶の形成や想起を担う司令塔である．大人になってからでも，学習などで脳の活動を高めることにより，この神経細胞が増え，脳力・記憶力が補強されることが期待される．

記憶にかかわる海馬では，どんなに歳をとっても新しくニューロンが生まれ続けている[1)2)]．新生ニューロンは，古くからあるニューロンと比べ，神経刺激に対する高い可塑性を有しており[3)]，記憶の形成にかかわっていると考えられている．これまでの研究から，学習行動などで海馬の活動が高まると新生ニューロンの数が増加することが示唆されてきたが[4)]，新生ニューロンが生まれる過程に学習行動そのものがどのように関与しているかについて，全く不明であった．

それでは，成体の海馬において，新生ニューロンはどのような細胞からどういった過程を経て生み出されているのであろうか？ 分裂細胞を調べるために核酸アナログであるブロモデオキシウリジンを使った研究が展開されてきた．その結果，グリア細胞様の性質をもつ1型前駆細胞（神経幹細胞：Type-1細胞）から，ニューロンとしての性質を一部獲得した2型前駆細胞（ニューロン前駆細胞：Type-2細胞）が分化し，この細胞より新生ニューロンが生み出されていることがわかってきた（図1）[5)]．新生ニューロンは，歯状回で顆粒細胞として成熟し，海馬回路網に機能的に組込まれることが証明されている．

海馬回路の活動と海馬の前駆細胞との機能的なかかわりを調べるためには，細胞が生きた状態で前駆細胞を特定し，その活動を記録する必要があった．神経前駆細胞のマーカーであるネスチンのプロモーター制御下でGFPを発現するネスチン—GFPマウスを用いることで，これら前駆細胞を成体の急性脳スライス内で同定し，パッチクランプ法により電気的活動を測定することに成功した[5)]．そこで本研究では，この実験システムを用いて，まず海馬神経回路からの神経刺激が前駆細胞に伝わるかどうかについて検討を行った．さらに，このような刺激が新生ニューロンを生み出すシグナルとして機能していると仮定し，マウス個体を用いた評価を進めた．そしてわれわれは，学習などの際，海馬のニューロンが特殊なパターン（シータ波リズム：学習時に海馬に特徴的に現れるニューロン活動リズム）で発火することで，この刺激がType-2細胞に伝わり，新生ニューロンへの分化が促進されることを突き止めた[6)]．

Learning-dependent enhancement in adult hippocampal neurogenesis

Yusuke Tozuka/Tatsuhiro Hisatsune : Department of Integrated Biosciences, University of Tokyo（東京大学大学院新領域創成科学研究科先端生命科学専攻）

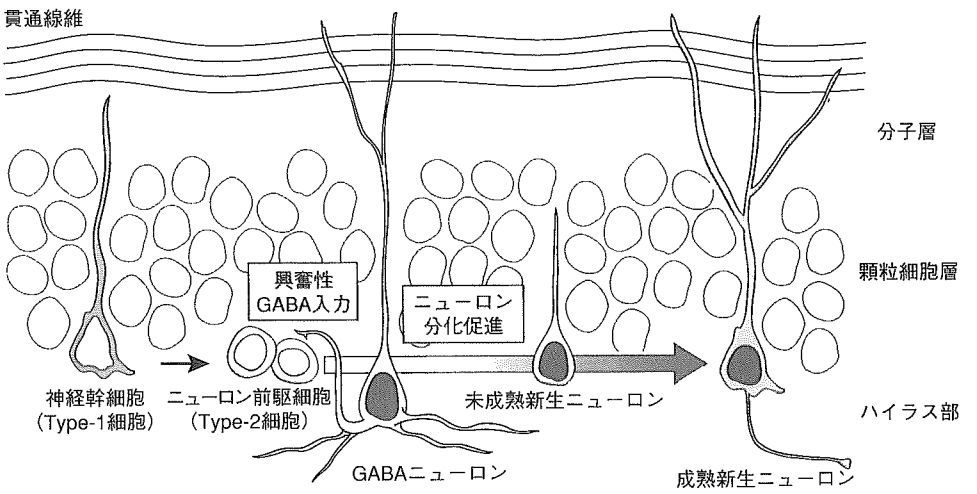

図1　成体海馬歯状回において新しくニューロンが生まれるまで
ラジアルグリア様の神経幹細胞（Type-1細胞）から，盛んに分裂を繰り返すニューロン前駆細胞（Type-2細胞）が発生する．貫通線維にシータ波が伝わるとGABAニューロンが興奮し，Type-2細胞はGABAニューロンから興奮性のGABA入力を受け取る．この入力によりニューロン分化が促進され，新生ニューロンへと成長し，海馬回路網に機能的に組込まれる

情報はシナプスを介して前駆細胞へと伝えられる

これまでの胎生期における研究から，分裂を繰り返す前駆細胞は周囲の回路との間に決してシナプス結合を形成することはないとされていたため[7)8)]，成体海馬前駆細胞が周囲の回路と直接コンタクトをしているかが非常に大きな問題であった．しかし海馬の活動が高まることで新生ニューロンの数が増加することから，われわれは海馬神経回路の活動が前駆細胞に働きかけることで，新たなニューロンが分化してくると考えた．

実験では，海馬スライスを用いて，Type-1細胞およびType-2細胞に対する海馬神経回路からの入力を調べた．Type-1細胞では神経伝達物質を介した神経入力は観察されなかったが，Type-2細胞ではGABA〔Gamma-Aminobutyric Acid：ガンマ-アミノ酪酸(ギャバ)〕を介したシナプス様入力が観察された．組織化学的な観察からも，GABAニューロンの末端がType-2細胞へ直接コンタクトしているという結果が得られた．分裂中の前駆細胞にシナプスがあるという報告はなく，きわめて新規性の高い発見となった[6)]．

また動物が学習行動をしているとき，海馬のGABAニューロンが特殊なパターン（シータ波リズム）で同期発火することが知られており，このシータ波が記憶の形成に非常に深くかかわっていると考えられている[9)]．興味深いことに，実験的にシータ波と同じ刺激を海馬の貫通線維（図1に表示）に加えると，GABAニューロンが興奮し，Type-2細胞へ刺激が伝達されることが明らかとなった[6)]．シナプスを介して，海馬前駆細胞は周囲の神経回路と一体となっており，海馬の活動情報をシグナルとして受け取っていることがはじめて明確に示された．

GABAで興奮：成体海馬においてニューロン分化を促進させるしくみ

では分裂を繰り返すType-2細胞へのGABA入力はどういった生理的効果をもたらすのか？ 通常成体脳内において，GABAは抑制性伝達物質として働いているが，われわれはGABA入力によりType-2細胞が脱分極することを明らかとした．これは，Type-2細胞が周囲のニューロンとは異なり，細胞内塩化物イオン濃度が高いことに起因している．このGABAによる脱分極は，引き続き電位依存性カルシウムチャネルを開口させ，細胞内へのカルシウム流入を誘起した．このカルシウム流入反応が引き金となり，ニューロン分化を誘導する転写因子（NeuroD）の発現量が増加し，ニューロン分化が誘導されることが明らかとなった[6)]

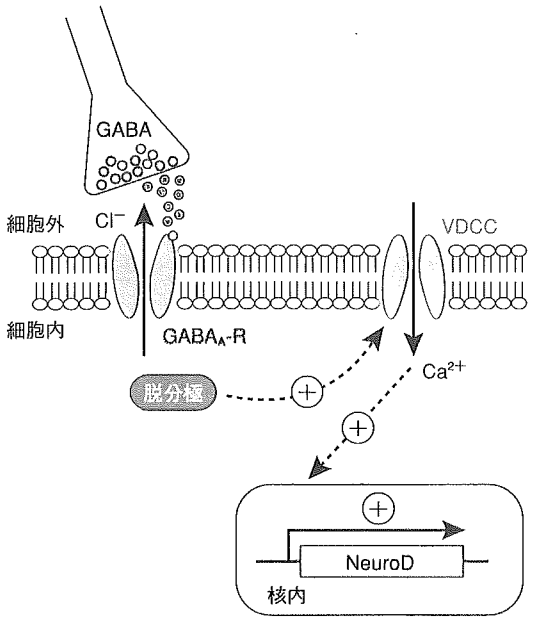

図2　興奮性GABA入力によるニューロン分化メカニズム
GABA入力により膜の脱分極が起こり，電位依存性カルシウムチャネルを介して，一過的にカルシウムイオンが流入する．この反応が引き金となり，ニューロン分化にかかわる転写因子（NeuroD）の発現量が増加する．GABA$_A$-R：A型GABA受容体，VDCC：電位依存性カルシウムチャネル

（図2）．

これまで，成体の海馬において，神経活動が高まることで回路網からグルタミン酸が放出され，これが前駆細胞に作用することで新生ニューロンへの分化が促進されているものと考えられてきた．しかし本研究から，前駆細胞への興奮性GABA入力がニューロン分化を促すシグナルとして働き，新生ニューロンの数を増やしていることが判明した（図1）．また実験的にシータ波を脳スライスに施すことで，GABAニューロンが刺激された．そして，このGABA性刺激を強化することで，前駆細胞から新生ニューロンへの分化が促進された．このような結果は，学習行動が刺激となって，結果的に新生ニューロンの数を増加させていることを強く示唆するものである．

おわりに

「成体海馬のニューロン新生」はヒトを含む成体哺乳類において保存されている脳のユニークな性質である．海馬は記憶機能にはじまり，抑うつ防止などの感情面に至るまで，幅広い働きをしている．新生ニューロンそのものが，記憶形成に関与することを示すデータも得られている[10]．そのため，いかに新生ニューロンの数を増やし，海馬の活動を高めることができるかについて，これまでにも精力的に研究が行われてきた．今回われわれは，海馬神経回路からの興奮性GABA入力がニューロンの新生を促進していることを突き止めた．今後，詳細にニューロン分化メカニズムや新生ニューロンの生理機能が解明されることで，記憶力の改善やうつ病に対する治療法の開発が期待できる．

文献

1）Eriksson, P. S. et al.：Neurogenesis in the adult human hippocampus. Nature Med., 4：1313-1317, 1998
2）van Praag, H. et al.：Functional neurogenesis in the adult hippocampus. Nature, 415：1030-1034, 2002
3）Schmidt-Hieber, C. et al.：Enhanced synaptic plasticity in newly generated granule cells of the adult hippocampus. Nature, 429：184-187, 2004
4）Drapeau, E. et al.：Spatial memory performances of aged rats in the water maze predict levels of hippocampal neurogenesis. Proc. Natl. Acad. Sci. USA, 100：14385-14390, 2003
5）Fukuda, S. et al.：Two distinct subpopulations of nestin-positive cells in adult mouse dentate gyrus. J. Neurosci., 23：9357-9366, 2003
6）Tozuka, Y. et al.：GABAergic excitation promotes neuronal differentiation in adult hippocampal progenitor cells. Neuron, 47：803-815, 2005
7）LoTurco, J. J. et al.：GABA and glutamate depolarize cortical progenitor cells and inhibit DNA synthesis. Neuron, 15：1287-1298, 1995
8）Demarque, M. et al.：Paracrine intercellular communication by a Ca^{2+}-and SNARE-independent release of GABA and glutamate prior to synapse formation. Neuron, 36：1051-1061, 2002
9）Buzsaki, G.：Theta oscillations in the hippocampus. Neuron, 33：325-340, 2002
10）Shors, T. J. et al.：Neurogenesis in the adult is involved in the formation of trace memories. Nature, 410：372-376, 2001

● 筆頭著者プロフィール ●

戸塚祐介：2002年，東京理科大学基礎工学部卒業．同年より，東京大学大学院新領域創成科学研究科に在籍し，久恒辰博助教授の指導を受ける．現在博士課程2年．進学以来，電気生理技術の習得に励み，『パッチマイスター』をめざす．成体脳におけるニューロン新生について，その生物学的意義の核心に迫るべくマウス？と格闘中．好きな言葉：「敵を知り己を知らば百戦危うからず」

Available online at www.sciencedirect.com

SCIENCE DIRECT®

Experimental Neurology 194 (2005) 1 – 11

Experimental Neurology

www.elsevier.com/locate/yexnr

Transplantation of GABAergic neurons into adult mouse neocortex

Dai Muramatsu, Yuki Sato, Sohei Hishiyama, Yusei Miyamoto, Tatsuhiro Hisatsune*

Department of Integrated Biosciences, University of Tokyo, Bioscience Building 402, 5-1-5 Kashiwanoha, Kashiwa, Chiba 277-8562, Japan

Received 1 September 2004; revised 17 December 2004; accepted 11 January 2005
Available online 30 March 2005

Abstract

GABAergic neurons in the neocortex contribute to various brain functions by regulating cortical pyramidal neurons. A deficiency of GABAergic neurons in the neocortex leads to the dysregulation of cortical neuronal circuits, but this can be overcome by cell transplantation, which provides a practical approach to repair damaged neuronal circuits. Here, we focused on the transplantation of committed neuronal progenitor cells. Because neuronal differentiation is considerably suppressed in the adult neocortex, we transfected proneural bHLH transcription factors into neural precursor cells to commit them to a neuronal lineage prior to the cell transplantation. We show that ventral neural stem cells transfected with Ngn1 are integrated as GABAergic neurons within a few days of transplantation into the adult mouse neocortex. These results demonstrate that the transplantation of committed neuronal progenitor cells is an effective method for brain repair.

Keywords: Neural progenitor cells; Adult mouse; GABAergic neurons; Cerebral cortex; bHLH transcription factors; Transplantation

Introduction

GABAergic interneurons in the neocortex form a part of neuronal ensembles that carry out functions such as sensory binding and memory formation (Buzsaki and Chrobak, 1995; Whittington et al., 1995). These functions are achieved by oscillating inhibitory networks which entrain large populations of pyramidal neurons (Buzsaki and Chrobak, 1995; Swadlow, 2003; Swadlow and Gusev, 2002). A deficiency of GABAergic interneurons is found in at least two major diseases in humans–epilepsy and ischemia (Schwartz-bloom and Sah, 2001)–leading to dysregulation of cortical neuronal circuit function. In adult mammalian brain tissue damaged by such diseases, the regeneration of cortical neurons cannot occur spontaneously. As such, transplantation of GABAergic interneurons may provide a promising therapeutic approach to repair damaged neuronal circuits in the neocortex.

Problems arise in determining what type of cells should be used to successfully carry out this treatment approach. Transplantation of primary cells from fetal CNS tissue has already been performed for the treatment of traumatic brain injury or Parkinson's disease (Bjorklund and Lindvall, 2000; Snyder et al., 2004) however the use of these primary cells for transplantation is controversial because of ethical issues and difficulties with cell preparation. Embryonic stem (ES) cells, mesenchymal stem cells, and other pluripotent cells may also be possible sources (Buzanska et al., 2002; Chen et al., 2001; Kim et al., 2002; Wernig et al., 2004; Wichterle et al., 2002), but risks associated with their use, such as the formation of teratoma, are yet to be overcome. Therefore, neural stem or progenitor cell lines have an advantage over fetal tissue and non-neuronal cells for cell replacement therapies (Snyder et al., 2004). Most neural stem or progenitor cell lines, however, do not differentiate into neurons in the adult neocortex since they do not have a definite lineage commitment. Thus, if it is possible to promote their neuronal fate in the adult neocortex, therapeutic transplantation of neural stem cell lines may become feasible. Here, we hypothesized that forced expression of proneural basic helix–loop–helix (bHLH) transcription factors in donor cells would enable more efficient neuronal differentiation, even when immature cells are transplanted into the adult mouse neocortex.

* Corresponding author. Fax: +81 4 7136 3632.
E-mail address: hisatsune@k.u-tokyo.ac.jp (T. Hisatsune).

0014-4886/$ - see front matter © 2005 Elsevier Inc. All rights reserved.
doi:10.1016/j.expneurol.2005.01.025

Proneural bHLH transcription factors, such as Ngn1, Ngn2, and Mash1, are known to affect fate determination and neuronal differentiation of neural stem cells (NSCs) (Johnson et al., 1990; Lee et al., 1997; Ma et al., 1996; Schuurmans and Guillemot, 2002; Ross et al., 2003). During brain development, these proneural bHLH transcription factors inhibit the differentiation of NSCs into glial cells and promote NSC differentiation into neurons (Nieto et al., 2001; Tomita et al., 2000). In this paper, we report that ventral NSCs transduced with Ngn1 show effective differentiation into GABAergic neurons in vitro. Furthermore, given the capacity of Ngn1 to induce neuronal differentiation of NSCs without changing their GABAergic fate, we transplanted Ngn1-transduced NSCs into the neocortex of adult mice to test the ability of these cells to integrate with the endogenous brain tissue. Surprisingly, the transplanted cells differentiated into neurons within just a few days of transplantation and showed GABAergic phenotype. These data indicate that, although the microenvironment in the adult neocortex would normally suppress the neuronal differentiation of transplanted cells, the suppression can be overcome by the forced expression of neurogenic factors in NSCs.

Materials and methods

Cell culture

Mouse striatal precursor-1 (MSP-1) cells, originating from a neural stem cell line established from ventral telencephalon tissue of p53 knockout mice (Yamada et al., 1999), were used. MSP-1 cells were plated on poly-ornithine/fibronectin-coated dishes in DMEM/F12 supplemented with N2 supplement containing basic fibroblast growth factor (basic-FGF) (10 ng/ml) and maintained in this manner overnight. Cells were cultured for 1 to 4 days following retrovirus infection (see below). Culture media were replaced with freshly prepared media every 2 days.

Virus production

The retrovirus vector plasmids pMY-IRES-EGFP and pMY-IRES-EGFP containing rat neurogenin1 and MASH1 coding regions were kindly provided by Dr. Kinichi Nakashima (Kumamoto University). Retroviruses were produced in a GP-293 packaging cell line (CLONTECH). Cells were transiently transfected at about 80% confluence with pVSV-G using TransFast Transfection Reagent (Promega). Supernatants were collected 48 h after transfection, filtered through 0.45 μm mixed cellulose ester filters (ADVANTEC), and concentrated by centrifuging at 6000 × *g* (16 h at 4°C). Pellets were suspended in DMEM/F12 supplemented with N2 supplement and stored at −80°C.

FACS analysis

Flow cytometric analyses were performed using a FACScan flow cytometer (Beckton Dickinson, San Jose, CA) as previously described (Yoshida et al., 2003). Cells from freshly collected tissue samples were resuspended at a density of 5×10^4 cells/50 ml in Ca^{2+}- and Mg^{2+}-free HBSS containing 0.1% BSA and 0.1% sodium azide and then mixed with a 1/25 dilution of biotin-conjugated monoclonal antibody (mAb) recognizing α_5 or β_1 integrin subunits (PharMingen, San Diego, CA) for 20 min on ice. Cell–mAb complexes were washed twice with Ca^{2+}- and Mg^{2+}-free HBSS containing 0.1% sodium azide and resuspended in a 1/50 dilution of streptavidin–phycoerythrin (st-PE) (PharMingen) for 20 min on ice. After washing once with Ca^{2+}- and Mg^{2+}-free HBSS containing 0.1% sodium azide, cells were resuspended in Ca^{2+}- and Mg^{2+}-free HBSS containing 0.1% BSA, 0.1% sodium azide, and 0.5 mg/ml propidium iodide (PI) (Wako). Dead cells were excluded by gating on the forward and side scatter plots and eliminating PI positive events.

Immunocytochemistry

Cultured cells were fixed with 4% paraformaldehyde (Wako) in PBS for 15 min at room temperature and then incubated for 2 h at room temperature in a PBS blocking solution containing 3% normal goat serum (Life Technologies) and 0.1% Triton X-100 (Wako). Incubation was continued overnight at 4°C in blocking solution containing 1/750 mouse anti-microtubule-associated protein-2ab (MAP-2a2b; neuron-specific marker), 1/1000 rabbit anti-Gad67 (Sigma) or 1/1000 mouse anti-NeuN (mature neuron specific marker), and 1/1000 rabbit anti-gamma-Aminobutyric acid (GABA) (Sigma). After washing 3 times with PBS, the cells were incubated for 2 h at room temperature in PBS containing 1/400 dilution of anti-mouse IgG rhodamine and 1/200 anti-rabbit Cy5 (Chemicon, Temecula, CA). Thereafter, cells were counterstained for 10 min in PBS containing 1 mg/ml DAPI (Sigma) and then mounted in DABCO/immunoblot. Labeled cells were analyzed by confocal scanning laser microscopy (Leica, Mannheim, Germany).

Electrophysiology

Whole-cell patch clamp recordings were performed on NSCs 4 days after infection with Ngn1-IRES-EGFP and/or control IRES-EGFP. For the recording of evoked sodium currents, cell membrane potential was held at −65 mV and stepped to +35 mV as described previously (Fukuda et al., 2003). The experimental chamber was perfused with artificial cerebrospinal fluid (ACSF) containing 124 mM NaCl, 2.5 mM KCl, 26 mM $NaHCO_3$, 10 mM glucose, 1.25 mM NaH_2PO_4, 2 mM $GaCl_2$, and 1

mM $MgCl_2$. Whole-cell patch electrodes were filled with a K-gluconate solution containing 120 mM potassium gluconate, 6 mM NaCl, 5 mM $CaCl_2$, 2 mM $MgCl_2$, 2 mM MgATP, 0.3 mM NaGTP, 10 mM EGTA, and 10 mM HEPES (pH 7.2). Tetrodotoxin (TTX; 1 mM) was applied and washed off cells using a custom-designed perfusion pipette positioned in close proximity to patched cells.

Cell preparation and transplantation

On the day of transplantation, the cell culture medium was replaced by Ca^{2+}- and Mg^{2+}-free HBSS, and thereafter by the same medium containing 10% trypsin for 5 min at 37°C. This was followed by bathing the cells in DMEM coating 10% FBS. Detached cells were transferred to a Falcon tube and centrifuged (5 min, 1400 rpm), resuspended, and counted in a hemocytometer and finally a suspension of 10,000 cells/μl in HBSS was prepared. Adult male and female ICR mice (4 weeks of age; purchased from Sankyo Lab Service Tokyo, Japan) were used as recipients. NSCs, transduced with Ngn1-IRES-EGFP, or control IRES-EGFP, were implanted into the neocortex via micropipettes (tip diameters approximately 100 μm). Cell suspensions were introduced in volumes of approximately 4 × 50 nl from a depth of 500–100 μm at intervals of 100 μm (total 200 nl per injection site at surface so that injection tracks spanned layers II/III through V. Each mouse received 1 μl of suspension in total (i.e., 10,000 cells) into the cortex. All mice receiving transduced NSCs transplants received daily injections of cyclosporine A (Shandimmun, Novartis, 10 mg/kg i.p.) and survived for 3–5 days. Mice were deeply anesthetized with ethyl ether and transcardially perfused with phosphate-buffered saline followed by phosphate-buffered 4% paraformaldehyde (pH 7.2–7.4) containing 30% sucrose. Brains were quickly removed and sectioned at 40 μm on a freezing microtome.

Immunohistochemistry

For analysis of grafted cells, one or two serial sections from each animal was incubated for 2 h at room temperature in a PBS blocking solution containing 3% normal goat serum (Life Technologies) and 0.3% Triton X-100 (Wako) and then overnight at 4°C with containing primary antibody consisting of 1/1000 rat anti-GFP (Nacalaiteque, INC) and 1/1000 mouse anti-NeuN (Chemicon, Temecula, CA) and/or 1/10000 rabbit anti-GFAP (DAKO, Glostrup, Dnemark), 1/100 goat anti-Doublecortin (Dcx; migrating immature neuron marker) (Santa Cruz biotechnology), 1/1000 rabbit anti-GABA (Sigma). After 3 washes with PBS, sections were incubated for 2 h at room temperature in PBS containing 0.3% Triton X-100 and secondary antibody, consisting of 1/1000 anti-rat IgG Alexa 488 (Molecular Probes) and 1/200 anti-mouse IgG Cy5 and 1/200 anti-rabbit or anti goat-Rhodamine (Chemicon, Temecula, CA). Thereafter, sections were counterstained for 10 min in PBS containing 1 mg/ml DAPI (Sigma) and mounted in DABCO/immunoblot. Labeled sections were analyzed using confocal scanning laser microscopy (Leica, Mannheim, Germany).

Results

Efficient neuronal commitment with the proneuronal gene, Ngn1

The neurogenic actions of Ngn1 and Mash1 on NSCs in vitro were compared. Mouse NSCs, retrovirally infected with Ngn1-IRES-EGFP, Mash1-IRES-EGFP, or control IRES-EGFP vectors, were cultured for 4 days in DMEM/F12 with N2 supplement containing basic-FGF, LIF/CNTF, or DMEM 10% FCS. Immunocytochemistry analysis (Fig. 1) showed that, while both Ngn1- and Mash1-infected NSCs generated neuronal cells that were immunopositive for NeuN (mature neuron specific marker), Ngn1-infected cells gave rise to a higher proportion of neuronally differentiated cells than did Mash1 (Fig. 1B). In contrast, control EGFP-infected cells were all immunonegative for NeuN, with most of them expressing GFAP (Fig. 1A).

We next investigated the effect of Ngn1 and Mash1 on neuronal and glial differentiation in the presence of LIF/CNTF or 10% FCS, which would normally induce the differentiation of virtually all kinds of NSCs into glial cells. Immunocytochemistry for glial cell markers GFAP revealed that no astrocytes were generated from Ngn1- or Mash1-infected cells, whereas many GFAP-positive cells were found in control EGFP-infected cultures. These results support previous studies showing that proneural bHLH transcription factors promote neuronal differentiation with cell cycle arrest and inhibit the differentiation of NSCs into glial cells (Nieto et al., 2001; Tomita et al., 2000).

Differentiation stage suitable for cell transplantation

In a previous study, we showed that a decrease of integrin $\alpha_5\beta_1$ subunit expression is indicative of NSC neuronal commitment (Yoshida et al., 2003). In addition, it was reported that cells close to maturation can be fragile and difficult to keep alive when transplanted (Fricker-Gates et al., 2002). In this context, cells in an early phase of neuronal differentiation might be capable of integration with neuronal cells after transplantation. To evaluate the time course of cell differentiation after Ngn1 transfection, we performed FACS analysis on MSP-1 cells transfected with either Ngn1-EGFP or control EGFP retrovirus. Representative FACS profiles shown in Fig. 2 for integrin

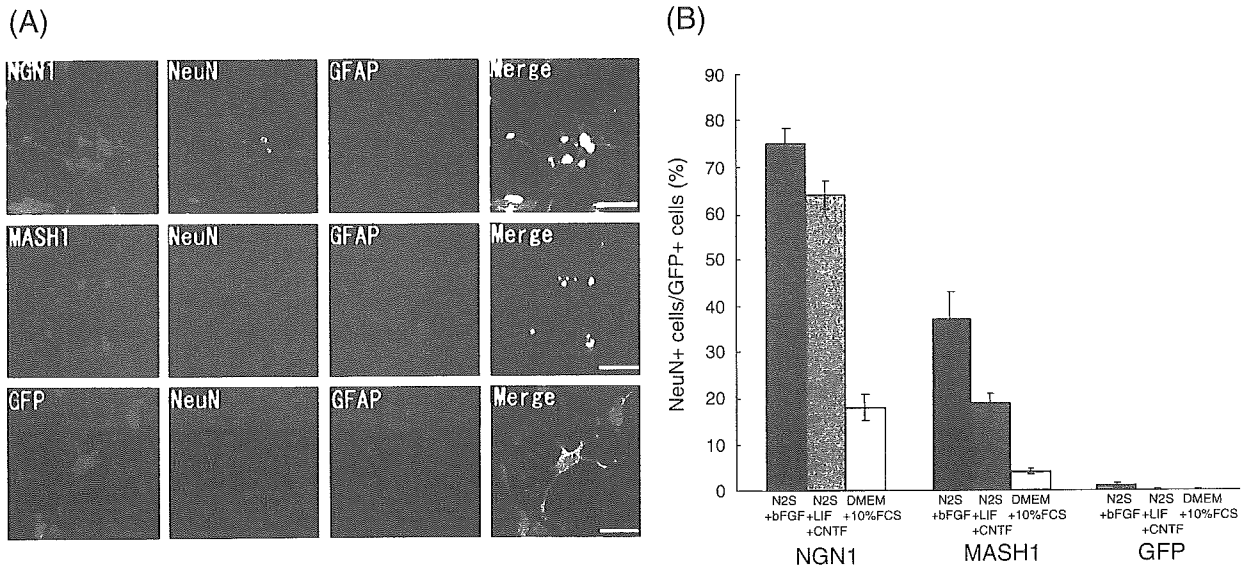

Fig. 1. Comparison of Ngn1 and Mash1 for inducing neuronal differentiation. (A) Cultures infected with the retroviruses encoding Ngn1-IRES-EGFP, Mash1-IRES-EGFP, or control EGFP were grown for 4 days in 10 ng/ml bFGF, 10 ng/ml LIF/CNTF, or DMEM 10% FCS and double-stained with antibodies to NeuN and DAPI. At day 4, Ngn1 and/or Mash1-infected cells express NeuN while control EGFP-infected cells express GFAP. (B) Average number of NeuN(+)/GFP(+) cells determined in 50 randomly selected 100× fields from four independent experiments carried out 4 days after retrovirus infection. Error bars represent standard deviations.

α_5 subunit levels from days 1–4 indicate that the integrin α_5 subunit expression started to decrease 2 days after the viral infection.

Immunocytochemistry was performed next to examine MAP-2a2b expression from days 1–4 in MSP-1 cells transfected with Ngn1-IRES-EGFP or control IRES-EGFP (Fig. 3). By day 2, Ngn1-infected cells had begun to change morphologically but did not express MAP-2 proteins. By day 3, these cells showed premature neuronal morphologies along with MAP-2

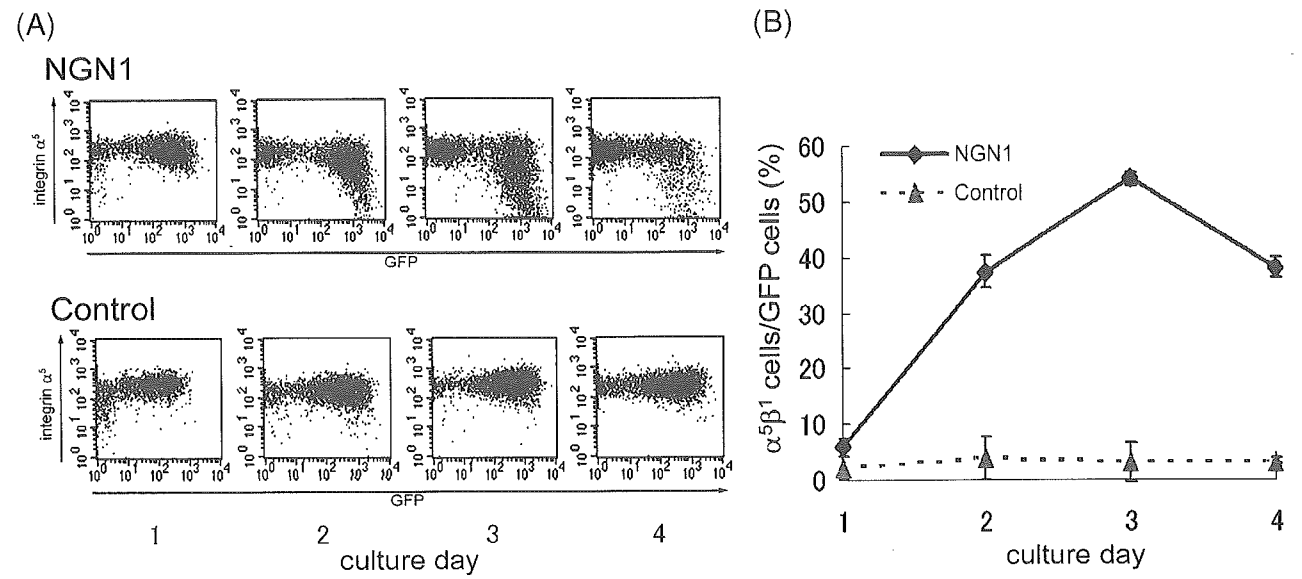

Fig. 2. Time course for neuronal commitment as evaluated by a decrease in integrin α_5 subunit expression. (A) The x axis represents the fluorescence intensity of GFP (Ngn1-IRES-EGFP, control IRES-EGFP) and y axis represents that of streptavidin phycoerythrin (st-PE). The decrease of integrin α_5 expression was observed in neural stem cells infected with Ngn1. A decrease in the proportion of integrin α5 subunits within the total population of Ngn1-infected neural stem cells during neural differentiation. The percentage values were obtained from FACS analysis by gating of Ngn1- control EGFP-infected cells. (B) The decrease in the proportion of integrin $\alpha^5\beta^1$ subunit expression within the total population of Ngn1-infected neural stem cells during neuronal differentiation. The percentage values were obtained from FACS analysis by gating of Ngn1, control EGFP-infected cells. Error bars represent standard deviations (n = 4).

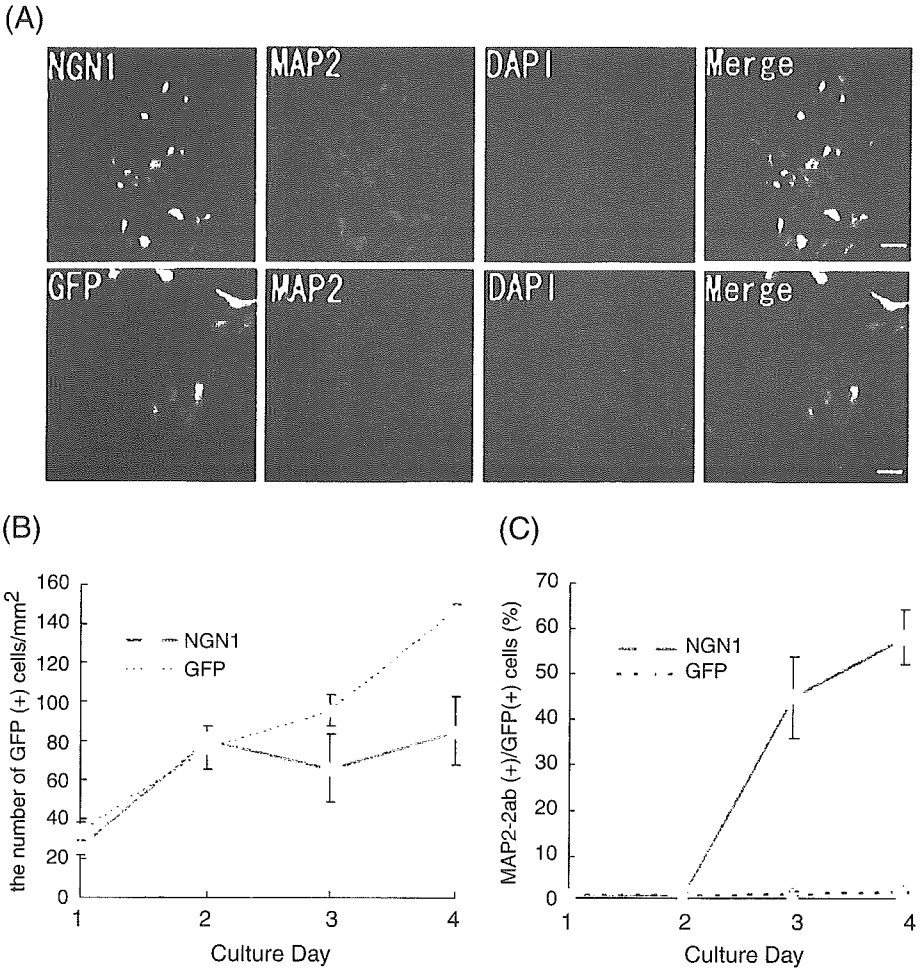

Fig. 3. Time course of neuronal maturation as evaluated by MAP-2 expression. (A) Cultures infected with Ngn1-IRES-EGFP or control IRES-EGFP retroviruses were grown for 4 days in 10 ng/ml bFGF, fixed, and double-stained with the antibodies to MAP-2a2b (neuron specific marker) and DAPI. Ngn1 and control IRES-EGFP are shown in green; MAP-2a2b in red; DAPI in blue. Scale bars = 20 μm. (B) Number of GFP-positive cells resulting from Ngn1-IRES-EGFP- and control EGFP-infected NSCs. Error bars represent standard deviations ($n = 4$). (C) Number of cells expressing MAP-2a2b in Ngn1-IRES-EGFP- and control EGFP-infected cells. Error bars represent standard deviations ($n = 4$). (For interpretation of the references to colour in this figure legend, the reader is referred to the web version of this article.)

expression. By day 4, the Ngn1-infected cells had adopted a neuronal morphology with round cell bodies and one or more long processes (Fig. 3). It can be concluded from these observations that day 2 cells are committed neuronal progenitor cells capable of maturing into neuronal cells and could thus be suitable for cell transplantation.

GABAergic phenotype of committed neuronal progenitor cells in vitro

Prior to cell transplantation, we confirmed the nature of the neuronal subtype induced in vitro by Ngn1. Double immunostaining with GABA or Gad67 and a neuronal marker performed 4 days after retrovirus infection clearly showed that most neurons generated from Ngn1-infection manifested GABAergic phenotype (Fig. 4). Whole-cell patch clamp experiments also demonstrated that Ngn1-transfected cells exhibited neuronal properties by day 4 (Fig. 5). From this, it can be inferred that Ngn1 preferentially induces differentiation of functional GABAergic neurons.

Integration of GABAergic neurons after cell transplantation

Committed neuronal progenitor cells derived from neural stem cells retrovirally infected with Ngn1-IRES-EGFP vector were cultured for 2 days in DMEM/F12 with N2 supplement containing basic-FGF and then transplanted into the neocortex of 4-week-old adult mice. Five days after transplantation, Ngn1-infected cells were distributed throughout the deeper and upper cortical layers

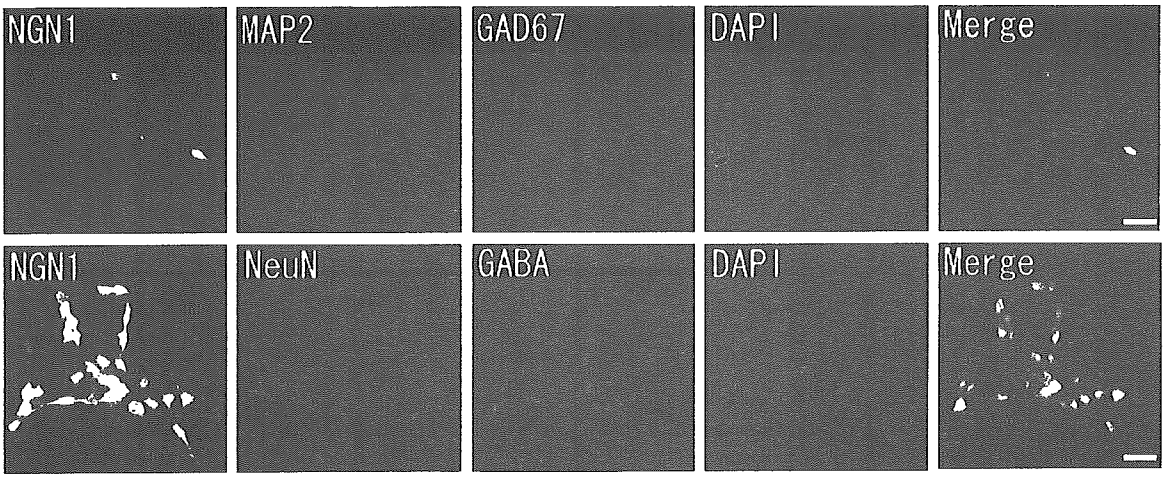

Fig. 4. Ngn1 induces formation of GABAergic neurons from ventral neural stem cells. Neural stem cells transfected with the Ngn1-IRES-EGFP were cultured in 10 ng/ml bFGF N2-S medium. After 4 days, the cells were fixed and double immunostaining was performed for Map2/Gad67 or NeuN/GABA. Data show that neurons induced from ventral neural stem cells by forced expression of proneural bHLH transcription factor Ngn1 were GABAergic phenotype.

of the neocortex in and/or around the injection sites. Many Ngn1-infected cells that had differentiated into smaller multipolar cells with interneuron-like morphologies could be at a distance greater than 40 μm from the injection site (Fig. 6). Immunofluorescent stainings showed that 26.6 ± 6.7 Ngn1-infected cells expressed NeuN (Figs. 6, 7A) and there were no GFAP (+) cells found (Fig. 7A). On the other hand, in the case of control EGFP, 398.9 ±59.6 cells showed astrocytic morphologies and expressed GFAP (Figs. 7A, C). The difference of total GFP (+) cells between two groups might be stemmed from the reduced proliferation activity of Ngn1-infected cells.

For further validation, we analyzed Ngn1-infected grafted cells inside and outside of the injection sites with anti-Dcx (migrating immature neuron marker) and anti-NeuN. As a result of immunofluorescent stainings, 83.5 ± 3.3% of the cells expressed Dcx and no NeuN (+) cells were found (Figs. 7B, C) inside of the injection sites where host NeuN (+) mature neurons were disrupted by the injection needle. Outside of injection sites, which means regions further than 40 μm from the injection sites, 15.8 ± 6.1% of the grafted cells expressed Dcx, the other 83.7 ± 7.7% expressed NeuN (Fig. 7B), and about 20% of the NeuN (+) cells faintly co-expressed Dcx (data not shown). These results may reflect the sequential neuronal differentiation of the transplanted Ngn1-infected cells. All the NeuN (+) cells (n = 16) were also positive for anti-GABA immunostaining (Fig. 7C), indicating that they differentiated into GABAergic phenotype within the adult neocortex. Moreover, the formation of spines on these neurons was observed at a higher magnification (Fig. 6), suggesting that grafted neurons formed synapses on host neurons within a short time after transplantation.

Discussion

Neurogenesis does not normally occur in the adult neocortex probably because non-neurogenic microenvironments prevent NSCs from differentiating into neurons. We therefore promoted the neuronal fate of NSCs by forced expression of proneural bHLH transcription factors to overcome the microenvironmental blockade. Indeed, while some neural stem cell lines (e.g. RN33B and C17.2) have a remarkable neurogenic capacity and differentiate into neurons after transplantation into adult neocortex (Shihabuddin et al., 1995; Snyder et al., 1997), this neurogenic property does not apply to most neural precursor cell lines (Whittemore and Snyder, 1996). In this communication, we show for the first time that a proneural gene, Ngn1, greatly promotes neuronal integration after cell transplantation into the neocortex of the adult mouse.

It has previously been shown that neuronal bHLH transcription factors, Ngn1 and Mash1, induce neuronal commitment in neural progenitor cells (Nieto et al., 2001; Sun et al., 2001; Tomita et al., 2000). Therefore, we initially compared Ngn1 with Mash1 in effectiveness for induction of the neuronal commitment. Contrary to the earlier speculation, our in vitro culture experiments demonstrated that Ngn1 was more effective than Mash1 for inducing the neuronal commitment in the NSCs. This issue would be supported from the previous studies using embryonal carcinoma P19 cells (Farah et al., 2000; Johnson et al., 1992; Kim et al., 2004).

During brain development, Ngn1 is expressed in dorsal progenitors in the telencephalon, which give rise to cortical glutamatergic pyramidal neurons (Schuurmans et al., 2004). However, there have been several studies implying that Ngn1 does not have strong function for specification

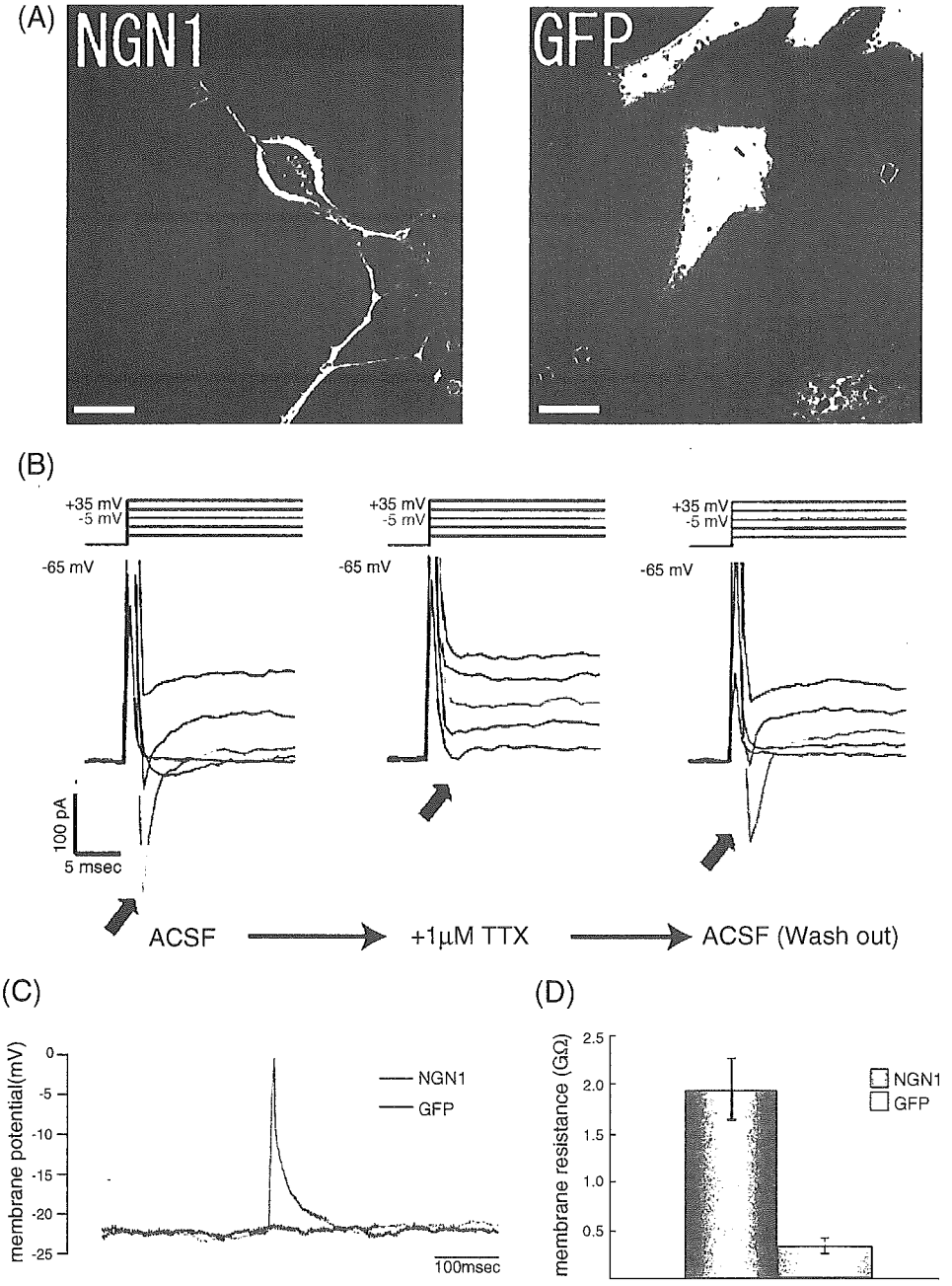

Fig. 5. Ngn1-infected neural stem cells exhibit neuron-like electrophysiological properties. Whole-cell current and voltage responses recorded from Ngn1-IRES-EGFP or control EGFP-infected neural stem cells at day 4. (A, B) To monitor fast inward currents, cells were stimulated in voltage-clamp mode by step depolarizations of 100 ms duration from a holding potential of −65 mV to a potential of +35 mV in 20 mV increments. TTX-sensitive, fast-rising inward currents (arrows) were evoked in Ngn1-infected cells. (C) A depolarizing current step of 80 pA for 15 ms evokes an action potential. (D) Examples of input resistance in Ngn1-IRES-EGFP and control EGFP-infected cells show that Ngn1-infected cells have a high membrane resistance similar to that of neurons. Error bars represent standard deviations (n = 4).

of glutamatergic phenotype (Fode et al., 2000; Parras et al., 2002). It can be postulated that Ngn1 would have a function rather for neuronal commitment than for neuronal phenotype specification. In this study, Ngn1-infected NSCs differentiated into GABAergic neurons in vitro and in vivo. This might be because we used neural stem cell line derived from ventral telencephalon, in which homeobox genes, Gsh1, Gsh2, and Dlx, are regionally expressed and would play a role in the specification of GABAergic neurons (Anderson et al., 1999; Fode et al., 2000; Parras et al., 2002; Yun et al., 2001; He et al., 2001). Thus, the induction of GABAergic neuronal specification of Ngn1-

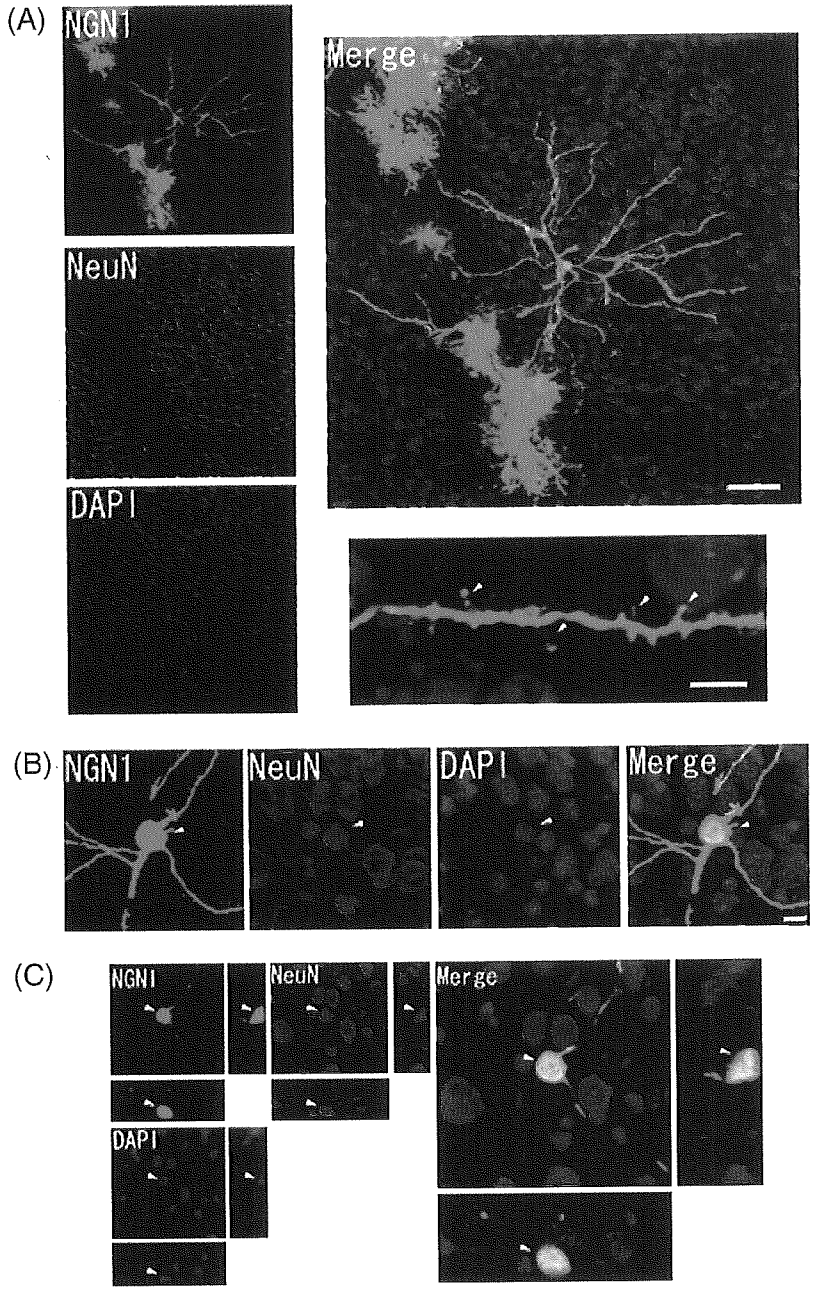

Fig. 6. Neuronal differentiation of transplanted neural stem cells was induced by Ngn1 in adult mouse cortex. Neural stem cells retrovirally infected with Ngn1-IRES-EGFP were transplanted into the adult mouse cortex and immunohistochemically detected 5 days later. (A) Cells with various morphologies were detected, among them cells with a neuronal profile. These cells expressed NeuN, which is a specific marker for mature neurons. Moreover, neuronal spines were frequently detected on the dendrites of these cells, indicating that Ngn1-IRES-EGFP (+) neurons had been integrated into the host neuronal circuitry. (B) A higher magnification image of a Ngn1-IRES-EGFP (+) neuron shows typical anti-NeuN staining with nuclear and cytoplasmic labeling (arrowheads). Nuclei of surrounding cells are stained with DAPI. (C) Confocal 3D reconstruction of the Ngn1-IRES-EGFP (+) neuron. Merging of the three individual images shows overlap of GFP (green), NeuN (red), and DAPI (blue) labeling (arrowheads). Scale bar = 40 μm, 8 μm (A), 4 μm (B).

infected progenitor cells shown in this study is probably due to these other transcription factors.

We characterized GABAergic neurons by neuronal morphologies and the immunostainings for anti-Gad67 and anti-GABA antibodies. However, recent studies have revealed the existence of the dual-phenotype GABA/glutamate neurons in several brain regions (Gutierrez et al., 2003; Ottem et al., 2004). For instance, hippocampal

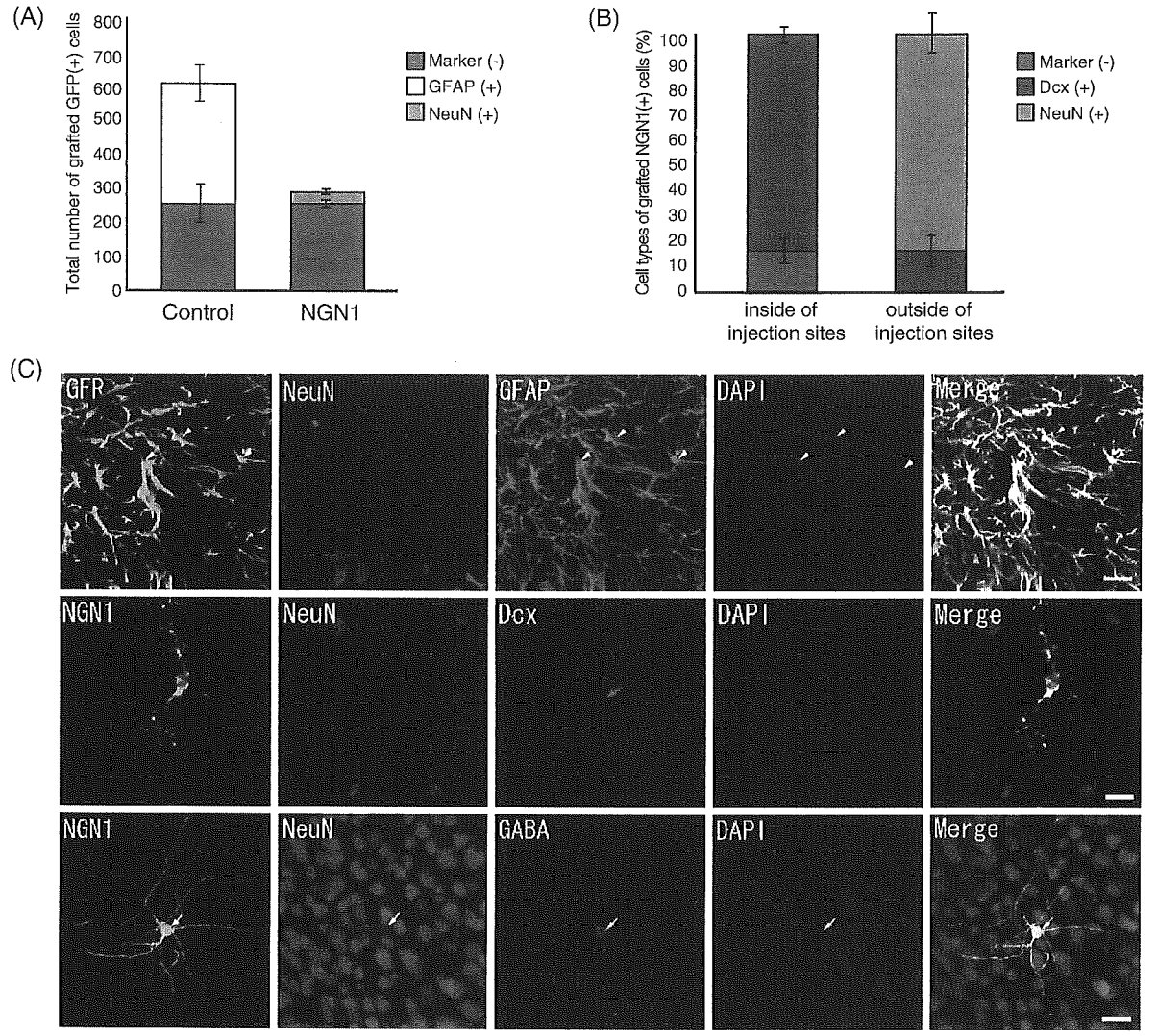

Fig. 7. GABAergic neurons in adult mouse cortex are induced by Ngn1-transfected neural stem cells. Neural stem cells grafted in the adult mouse cortex were analyzed by immunohistochemistry at 5 days post-transplantation. (A) Total number of cell types in grafted Ngn1-IRES- EGFP or control EGFP-infected cells. Triple-immunostaining for anti-GFP, NeuN, and GFAP with DAPI were performed on 20 sections containing grafted Ngn1 or control EGFP infected cells. Error bars represent standard deviation ($n = 4$). Marker (−) represents GFP^+, $NeuN^-$, and $GFAP^-$ cells. (B) Percentages of cell types of Ngn1 infected cells are counted inside and outside of the injection sites. Triple-immunostaining for anti-GFP, anti-Dcx, and anti-NeuN with DAPI were performed on 10 sections containing grafted Ngn1-infected cells. Inside of the injection sites are defined as areas where host NeuN (+) mature neurons are disrupted by the needle tracts. Outside of injection sites are defined as areas further than 40 μm from injection sites. In these areas, host intact NeuN (+) mature neurons densely exist. Error bars represent standard deviation ($n = 4$). Marker (−) represents GFP^+, Dcx^-, and $NeuN^-$ cells. (C) Immunostained images in the first row show that control EGFP infected neural stem cells were mostly differentiated into GFAP (+) astrocytes (arrowheads). The second row shows that grafted Ngn1-infected cells expressed Dcx. In the third row, it is shown that grafted Ngn1-infected cells express NeuN and are immunopositive for anti-GABA antibody. Triple-immunostaining for anti-GFP, NeuN, and GABA with DAPI were performed on 10 sections containing grafted Ngn1-infected cells. It is confirmed that all NeuN (+) cells are immunopositive for GABA. Scale = 20 μm.

granule cells, which had been considered to be glutamatergic, also showed GABAergic phenotypes (Gutierrez et al., 2003). Therefore, although the cells transplanted here showed GABAergic phenotypes, it might still have possibility of bearing glutamatergic properties as well. For the present, further investigations are required to clarify this issue.

Interestingly, we also identified spine formation just 3 days after transplantation. These results indicate that NSCs with forced expression of Ngn1 differentiated into functional mature neurons rapidly and were then integrated into host neuronal circuits. Given that it has been suggested that 1 month is required for transplanted NSCs to be integrated into host circuits (Englund et al., 2002; Shihabuddin et al., 1995; Snyder et al., 1997), our method may make neuronal cell transplantation into the adult mouse neocortex and/or other brain areas faster and easier than before.

Acknowledgments

We thank Dr. Ron McKay for his help in the initial phase of this study, Dr. Jeff Macklis for help with the cell transplantation, and Dr. Kinichi Nakashima for providing viral vectors.

References

Anderson, S., Mione, M., Yun, K., Rubenstein, J.L.R., 1999. Differential origins of neocortical projection and local circuit neurons: role of Dlx genes in neocortical interneurogenesis. Cereb. Cortex, 9, 646–654.

Bjorklund, A., Lindvall, O., 2000. Cell replacement therapies for central nervous system disorders. Nat. Neurosci., 3, 537–544.

Buzanska, L., Machaj, E.K., Zablocka, B., Pojda, Z., 2002. Human cord blood-derived cells attain neuronal and glial features in vitro expression of neural markers in human umbilical cord blood. J. Cell Sci., 115, 2131–2138.

Buzsaki, G., Chrobak, J.J., 1995. Temporal structure in spatially organized neuronal ensembles: a role for interneuronal networks. Curr. Opin. Neurobiol., 5, 504–510.

Chen, J., Sanberg, P.R., Li, Y., Wang, L., Lu, M., Willing, A.E., Sanchez-Ramos, J., Chopp, M., 2001. Intravenous administration of human umbilical cord blood reduces behavioral deficits after stroke in rats. Stroke, 32, 2682–2688.

Englund, U., Bjoklund, A., Wictorin, K., Lindvall, O., Kokaia, M., 2002. Grafted neural stem cells develop into functional pyramidal neurons and integrate into host cortical circuitry. Proc. Natl. Acad. Sci. U. S. A., 26, 17089–17094.

Farah, M.H., Olson, J.M., Sucic, H.B., Hume, R.I., Tapscott, S.J., Turner, D.L., 2000. Generation of neurons by transient expression of neural bHLH proteins in mammalian cells. Development, 127, 693–702.

Fode, C., Ma, Q., Casarosa, S., LeMeur, M., Dierich, A., Ang, S.L., Anderson, D.J., Guillemot, F., 2000. A role for neural determination genes in specifying the dorsoventral identity of telencephalic neurons. Genes Dev., 14, 67–80.

Fricker-Gates, R.A., Shin, J.J., Tai, C.C., Catapano, L.A., Macklis, J.D., 2002. Late-stage immature neocortical neurons reconstruct interhemispheric connections and form synaptic contacts with increased efficiency in adult mouse cortex undergoing targeted neurodegeneration. J. Neurosci., 22, 4045–4056.

Fukuda, S., Kato, F., Tozuka, Y., Yamaguchi, M., Miyamoto, Y., Hisatsune, T., 2003. Two distinct subpopulations of nestin-positive cells in adult mouse dentate gyrus. J. Neurosci., 23, 9357–9366.

Gutierrez, R., Romo-Parra, R., Maqueda, J., Vivar, C., Ramirez, M., Morales, M.A., Lamas, M., 2003. Plasticity of the GABAergic phenotype of the "glutamatergic" granule cells of the rat dentate gyrus. J. Neurosci., 23, 5594–5598.

He, W., Ingraham, C., Rising, L., Goderie, S., Temple, S., 2001. Multipotent stem cells from the mouse basal forebrain contribute GABAergic neurons and oligodendrocytes to the cerebral cortex during embryogenesis. J. Neurosci., 21, 8854–8862.

Johnson, J.E., Birren, S.J., Anderson, D.J., 1990. Two rat homologues of *Drosophila* achaete-scute specifically expressed in neuronal precursors. Nature, 346, 858–861.

Johnson, J.E., Zimmerman, T., Saito, T., Anderson, D.J., 1992. Induction and repression of mammalian achaete-scute homologue (MASH) gene expression during neuronal differentiation of P19 embryonal carcinoma cells. Development, 114, 75–87.

Kim, J.H., Auerbach, J.M., Rodriguez-Gomez, J.A., Velasco, I., Gavin, D., Lumelsky, N., Lee, S.H., Nguyen, J., Sanchez-Pernaute, R., 2002. Dopamine neurons derived from embryonic stem cells function in an animal model of Parkinson's disease. Nature, 418, 50–56.

Kim, S., Yoon, Y.S., Kim, J.W., Jung, M., Kim, S.U., Lee, Y.D., Suh-Kim, H., 2004. Neurogenin1 is sufficient to induce neuronal differentiation of embryonal carcinoma P19 cells in the absence of retinoic acid. Cell. Mol. Neurobiol., 24, 343–356.

Lee, J.E., Price, J., Thurlow, L., 1997. Basic helix–loop–helix genes in neural development. Curr. Opin. Neurobiol., 7, 13–20.

Ma, Q., Kintner, C., Anderson, D.J., 1996. Identification of neurogenin, a vertebrate neuronal determination gene. Cell, 87, 43–52.

Nieto, M., Schuurmans, C., Britz, O., Guillemot, F., 2001. Neural bHLH genes control the neuronal versus glial fate decision in cortical progenitors. Neuron, 29, 401–403.

Ottem, E.N., Godwin, J.G., Krishnan, S., Petersen, S.L., 2004. Dual-phenotype GABA/Glutamate neurons in adult preoptic area: sexual dimorphism and function. J. Neurosci., 24, 8097–8105.

Parras, C.M., Schuuramans, C., Scardigli, R., Kim, J., Anderson, D.J., Guillemot, F., 2002. Divergent functions of the proneural genes Mash1 and Ngn2 in the specification of neuronal subtype identity. Genes Dev., 16, 324–338.

Ross, S.E., Greenberg, M.E., Stiles, C.D., 2003. Basic helix-loop-helix factors in cortical development. Neuron, 39, 13–25.

Schuurmans, C., Guillemot, F., 2002. Molecular mechanisms underlying cell fate specification in the developing telencephalon. Curr. Opin. Neurobiol., 12, 26–34.

Schuurmans, C., Armant, O., Nieto, M., Stenman, J.M., Britz, O., Kienin, N., Langevin, L.-M., Seibt, J., Brown, C., Tang, H., Cunningham, J.M., Dyck, R., Walsh, C., Campbell, K., Polleux, F., Guillemot, F., 2004. Sequential phase of neocortical fate specification involved neurogenin-dependent and -independent pathways. EMBO J., 23, 2892–2902.

Schwartz-bloom, R.D., Sah, R., 2001. gamma-aminobutyric acid(A) neurotransmission and cerebral ischemia. J. Neurochem., 77, 353–371.

Shihabuddin, L.S., Hertz, J.A., Holets, V.R., Whittemore, S.R., 1995. The adult CNS retains potential to direct region -specific differentiation of a transplanted neuronal precursor cell line. J. Neurocsci., 15, 6666–6678.

Snyder, E.Y., Yoon, C., Flax, J.D., Macklis, J.D., 1997. Multipotent neural precursors can differentiate toward replacement of neurons undergoing targeted apoptic degeneration in adult mouse neocortex. Proc. Natl. Acad. Sci., 94, 11663–11668.

Snyder, E.Y., Daley, G.Q., Goodell, M., 2004. Taking stock and planning for the next decade: realistic prospects for stem cell therapies for the nervous system. J. Neurosci. Res., 76, 157–168.

Sun, Y., Nadal-Vicens, M., Misono, S., Lin, M.Z., Zubiaga, A., Hua, X., Fan, G., Greenberg, M.E., 2001. Neurogenin promotes neurogenesis and inhibits glial differentiation by independent mechanisms. Cell, 104, 365–376.

Swadlow, H.A., 2003. Fast-spike interneurons and feedforward inhibition in awake sensory neocortex. Cereb. Cortex, 13, 25–32.

Swadlow, H.A., Gusev, A.G., 2002. Receptive-field construction in cortical inhibitory interneurons. Nat. Neurosci., 5, 403–404.

Tomita, K., Moriyoshi, K., Nakanishi, S., Guillemot, F., Kageyama, R., 2000. Mammalian achaete-scute and atonal homologs regulate neuronal versus glial fate determination in the central nervous system. EMBO J., 20, 5460–5472.

Wernig, M., Benninger, F., Schmandt, T., Rade, M., Tucker, K.L., Bussow, H., Beck, H., Brustle, O., 2004. Functional integration of embryonic stem cell-derived neuron in vivo. J. Neurosci., 24, 5258–5268.

Whittemore, S.R., Snyder, E.Y., 1996. Physiological relevance and functional potential of central nervous system-derived cell lines. Mol. Neurobiol., 12, 13–38.

Whittington, M.A., Traub, R.D., Jefferys, J.G.R., 1995. Synchronized oscillation in interneuron networks driven by metabotropic glutamate receptor activation. Nature, 373, 612–615.

Wichterle, H., Lieberma, I., Porter, J.A., Jessell, T.M., 2002. Directed differentiation of embryonic stem cells into motor neurons. Cell, 110, 385–397.

Yamada, K., Hisatsune, T., Uchino, S., Nakamura, T., Kudo, Y.,

Kaminogawa, S., 1999. NMDA receptor mediated Ca2+ responses in neurons differentiated from p53−/− immortalized murine neural stem cells. Neurosci. Lett., 264, 165–167.

Yoshida, N., Hishiyama, S., Yamaguchi, M., Hashiguchi, M., Miyamoto, Y., Kaminogawa, S., Hisatsune, T., 2003. Decrease in expression of alpha 5 beta 1 integrin during neuronal differentiation of cortical progenitor cells. Exp. Cell Res., 287, 262–271.

Yun, K., Potter, S., Rubenstein, J.L.R., 2001. Gsh2 and Pax6 play complementary role in dorsoventral patterning of the mammalian telencephalon. Development, 128, 193–205.